The
ENGINEERS' DIGEST

REVIEW OF ENGINEERING PROGRESS ABROAD

VOL. IV. No. 7 JULY, 1943

CHURCHILL CENTRELESS GRINDING MACHINES.
Built for precision work and continuous high production.

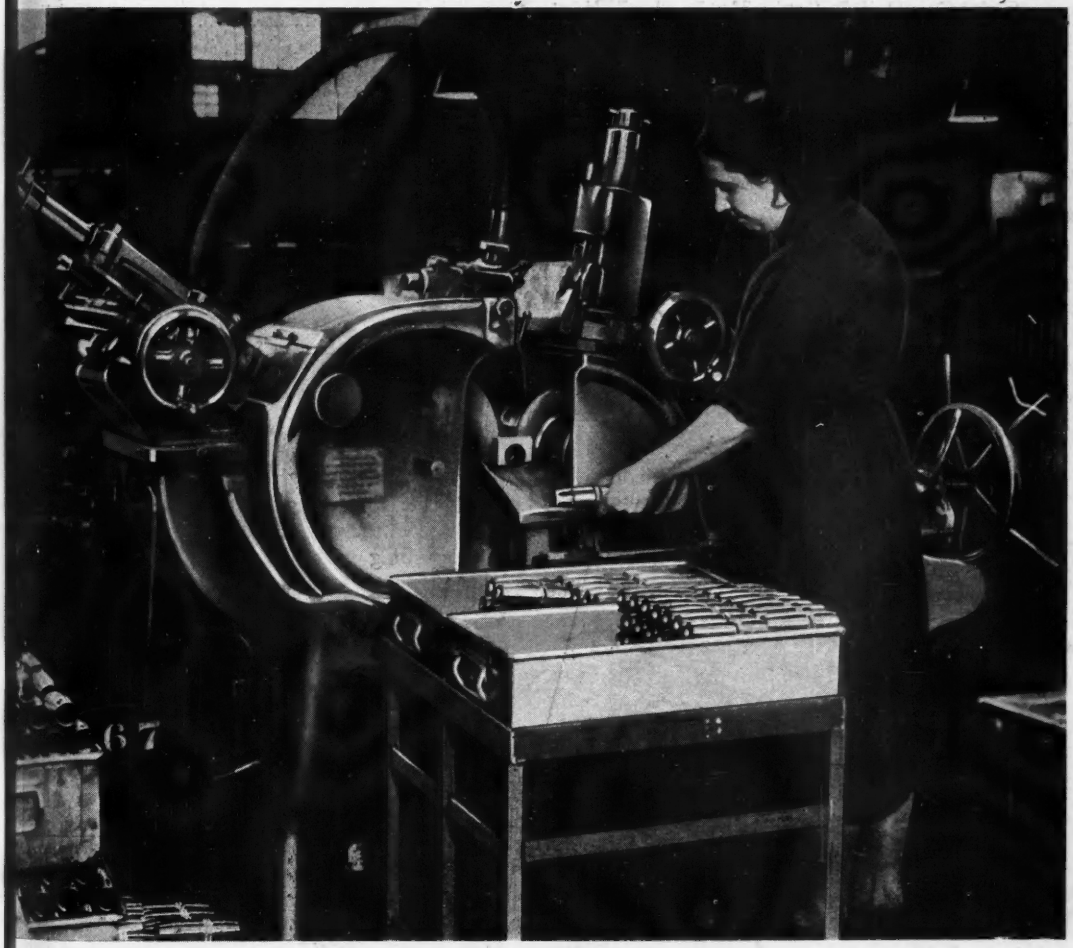

THE CHURCHILL MACHINE TOOL CO. LTD., BROADHEATH, Nr. MANCHESTER

THE ENGINEERS' DIGEST

REVIEW OF ENGINEERING PROGRESS ABROAD

Published Monthly at 120, Wigmore Street, London, W. 1.

Publishers : **ENGINEERS' DIGEST LTD.** - - - - Telephone : WELBECK 9357

Advertisement Dept. - 120, Wigmore Street, London, W.1 - Telephone : Welbeck 9357

Distribution - - E. & F. N. SPON, LTD., 57, Haymarket, London, S.W.1
Telephone : Whitehall 1860. Telegrams : Fenspon, Lesquare, London

Editorial Dept. - - 120, Wigmore Street, London, W.1 - Telephone : Welbeck 9357

Subscriptions to : ENGINEERS' DIGEST LTD., 120, Wigmore Street, London, W.1, or
E. & F. N. SPON, LTD., 57, Haymarket, London, S.W.1

ANNUAL SUBSCRIPTION OF 12 NUMBERS, £2 2s. SINGLE COPIES, 4s. 6d.

ADVISORY COMMITTEE

J. F. ALCOCK, B.A., A.M.I.Mech.E.
R. W. ALLOTT, M.A., A.R.Ae.S.
E. ALTON, D.Eng., A.M.Inst.B.E.
H. H. ASBRIDGE, M.B.E., M.I.Mech.E.
R. W. AYERS, M.I.W.
Col. J. BOWDEN, M.Inst.C.E., M.I.Mech.E.
H. H. BROUGHTON, M.I.Mech.E.
F. BUCKINGHAM, B.Sc., A.M.Inst.C.E., A.M.I.Mech.E., [A.M.I.E.E.
T. H. BURNHAM, B.Sc. (Lond.), A.M.I.Mech.E.
J. S. CASWELL, M.Sc., M.I.Mech.E.
G. C. SAFFERY COOPER.
J. DICK, Ph.D., B.Sc., A.M.I.Mech.E.
D. FIFE, M.I.Mech.E.
G. E. FOXWELL, D.Sc. (Lond.), F.Inst.P., F.Inst.F., M.Inst. [Gas.E.
R. GRIFFITHS, M.Sc.
H. HEYWOOD, Ph.D., M.Sc. (Eng.), A.M.I.Mech.E.
O. HURST, M.Inst.N.A.
Capt. J. S. IRVING, M.I.Mech.E., M.I.A.E., A.F.R.Ae.S., M.S.A.E.
F. C. JOHANSEN, M.Sc. (Eng.), M.I.Mech.E., F.R.Ae.S., M.I.Loco.E.
W. J. KEARTON, D.Eng., M.I.Mech.E., A.M.Inst.N.A.
Prof. W. KERR, Ph.D., M.I.Mech.E.
G. V. LOMONOSOFF, Dr.Ing., M.I.Mech.E.
B. J. LYMER, M.I.Mech.E.
D. T. MacIVOR, M.I.Mech.E., M.Cons.E.
W. O. MANNING, F.R.Ae.S.
R. B. MATTHEWS, Wh.Ex., A.M.Inst.C.E., M.I.E.E., F.R.Ae.S.
Prof. A. L. MELLANBY, D.Sc., LL.D., M.I.Mech.E.
J. H. R. RATCLIFF, B.Sc. (Eng., Hons.), M.I.Mech.E.
Col. C. W. D. ROWE.
W. A. SCOBLE, D.Sc., A.R.C.Sc., M.I.Mech.E.
P. W. SEEWER, D.E. (Zurich), M.Inst.C.E., M.I.Mech. E.
Prof. S. PARKER SMITH, D.Sc., M.I.E.E., A.M.Inst.C.E.
C. E. H. VERITY, A.M.Inst.C.E., A.M.I.E.E., A.M.I.Mech.E.
E. G. WALKER, F.C.G.I., B.Sc. (Eng.), M.Inst.C.E., M.I.Mech.E., M.Am.Soc.C.E.
Major F. L. WATSON, M.Inst.C.E., M.I.Mech.E.
G. WATSON, M.Inst.C.E., M.I.Mech.E.
C. H. WOODFIELD, M.I.Mech.E., M.I.Struct.E.
T. WRIGHT, Ph.D., M.Sc.
M. L. YATES, M.Sc.Tech., M.A. (Com.), M.I.Mech.E.

"CRONITE" is the Nickel Chromium Alloy of highest commercial grade. "CRONITE" castings find employment in almost every branch of the engineering industry replacing iron or steel for heat resisting purposes. There is no structural breakdown with the alloy, retention of shape being maintained almost to melting point.

Typical Uses at 800° Centigrade and over.

CASEHARDENING VESSELS.
ROTATING CARBURIZING RETORTS.
LEAD POTS.
SALT BATH VESSELS.
MUFFLES AND FURNACE PARTS.
FURNACE HEARTH PLATES.
GLASS BLOWER NOZZLES.
PYROMETER PROTECTION SHEATHS.

THE CRONITE FOUNDRY CO. LTD.
Lawrence Rd., Tottenham, London N15.
Telephone: STAMFORD HILL 4237

T

: 9357
: 9357

: 9357

6d.

R.Ae.S.

ch.E.
oc.C.E.

7

Back
Desi
Dire
Elec
Engi
Free
Hyd
The
The
Prac
Sur
The

CONTENTS

	page
Back Axle Drive or All Wheel Drive for Heavy Lorry with Trailer "*The Engineers' Digest*," *Vol.* 4, *No.* 7, *p.* 216.	216
Design of D.C. Magnets "*The Engineers' Digest*," *Vol.* 4, *No.* 7, *p.* 202.	202
Direct Pneumatic Hammer Riveting in Aircraft Production "*The Engineers' Digest*," *Vol.* 4, *No.* 7, *p.* 196.	196
Electronic Elimination of Oil Mists "*The Engineers' Digest*," *Vol.* 4, *No.* 7, *p.* 205.	205
Engine Cooling Problems Arising in Motor Car Design (Part II.) "*The Engineers' Digest*," *Vol.* 4, *No.* 7, *p.* 210.	210
Freezing of Acids in Accumulators "*The Engineers' Digest*," *Vol.* 4, *No.* 7, *p.* 200.	200
Hydraulic Turbine Practice of the T.V.A. "*The Engineers' Digest*," *Vol.* 4, *No.* 7, *p.* 193.	193
The Influence of Reynolds' Number at High Mach Numbers "*The Engineers' Digest*," *Vol.* 4, *No.* 7, *p.* 199.	199
The Influence of Riveting Tools on the Driving of Heat-Treated Light Metal Rivets "*The Engineers' Digest*," *Vol.* 4, *No.* 7, *p.* 197.	197
Practical Turbine Lubrication "*The Engineers' Digest*," *Vol.* 4, *No.* 7, *p.* 194.	194
Surface Currents on Plastics "*The Engineers' Digest*," *Vol.* 4, *No.* 7, *p.* 207.	207
The Zeiss-Ikon Slow-Motion Camera "*The Engineers' Digest*," *Vol.* 4, *No.* 7, *p.* 215.	215

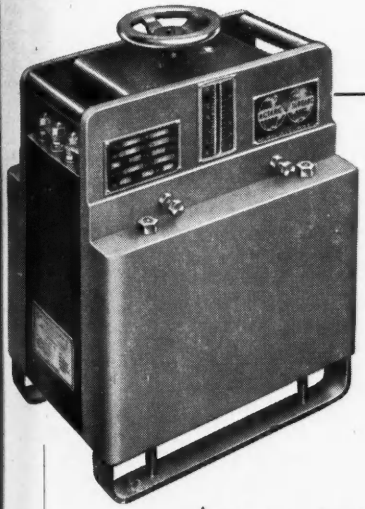

Applied Science

THE most advanced principles of welding transformer design are built into the Actarc Welding plant. The illustration shows the Actarc "Monta" which has the following important advantages:—

- **15—200 AMPS**
- **INFINITELY VARIABLE**
- **WEIGHS ONLY 175 LBS.**

★ On and after 1st February, applications for purchase certificates for Welding Plant should be submitted to the Machine Tool Control Regional Director, and not to the Machine Tool Control Headquarters.

ACTARC SUREARC

ARC MANUFACTURING CO., LTD.

PROPRIETORS OF THE SURE-ARC ELECTRODE CO. LTD.

ACTARC WORKS, GOLDHAWK ROAD, LONDON W.12

REGD. TRADE MARK

TELEPHONE: SHE 1151/3 (Private Branch Exchange). TELEGRAMS: ACTIVARC, PHONE, LONDON. CABLES: ACTIVARC, LONDON.

189

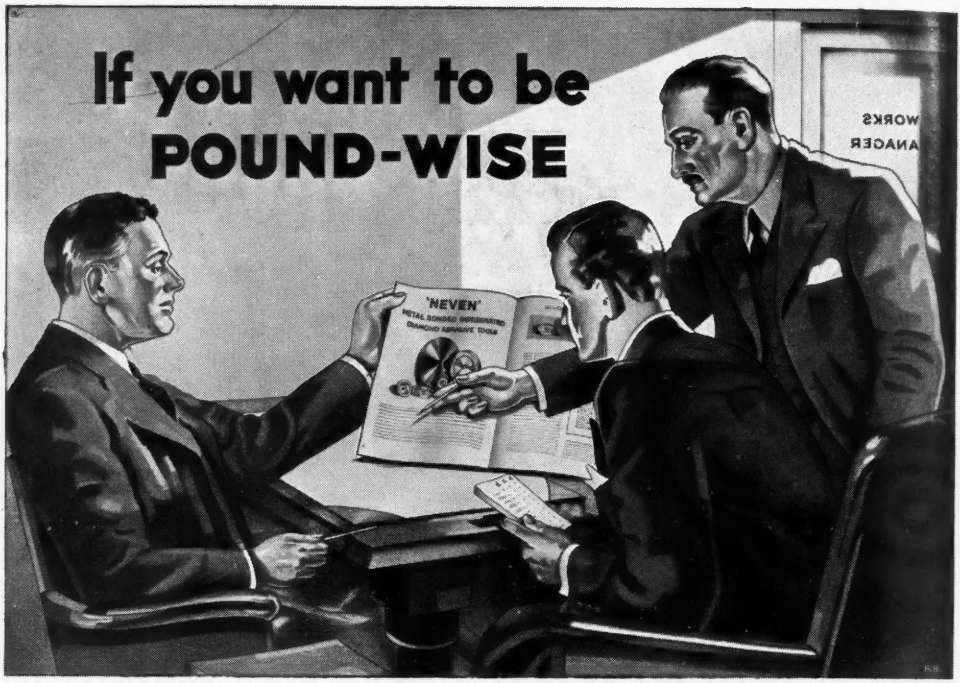

-You should NEVENISE!

'NEVEN' METAL BONDED IMPREGNATED DIAMOND GRINDING WHEELS.

'Neven' metal bonded abrasive wheels are impregnated with carefully selected diamond grains of uniform size to ensure perfect finish with maximum efficiency. The 'Neven' wheel will remove in the same time and at a greatly reduced cost, 5 to 6 times the amount of carbide than would be removed with a silicon carbide wheel. A diamond wheel cannot be rectified and must maintain an absolutely plain grinding surface. Every 'Neven' wheel will grind or recondition thousands of tools. The tools will not only last longer with less regrinds but give longer and more efficient service.

Single or double sided wheels availabe in 3", 4", 5", 6", 8", 10" and 12" diameter.

'NEVEN' CHIP GROOVING WHEELS available in 3", 6" and 8" diameter.

'NEVEN' IMPREGNATED DIAMOND CUTTING DISCS.

These cutting discs are ideal for the sawing of all hard or abrasive materials. They are specially suitable for the cutting of metallic carbides and materials of a similar hardness and supersede the abrasive cutting off wheel.

Available in 3", 6", 8", 10" and 12" diameter.

'NEVEN' DIAMOND HAND LAPS.

These are used for final lapping all carbide tools and are specially recommended for finishing Wimet brand tools, reamer blades, and other metals requiring a super finish. They are also invaluable for retouching tool set-ups in machines, obviating the necessity of re-assembling. Particulars of the complete range sent on request.

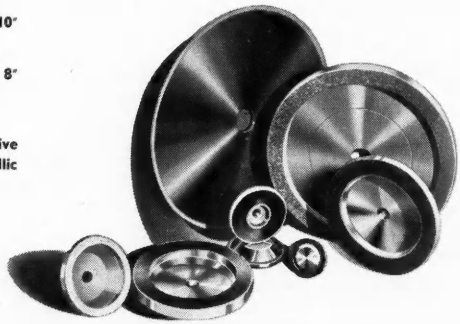

A.C. Wickman LIMITED
• COVENTRY • ENGLAND •

LONDON BRISTOL BIRMINGHAM MANCHESTER LEEDS GLASGOW NEWCASTLE

HYDRAULIC TURBINE PRACTICE OF THE T.V.A.

By H. J. PETERSEN and J. F. ROBERTS. (From *Mechanical Engineering*, Vol. 65, No. 4, April, 1943, pp. 237-244).

THE hydraulic-power system of the Tennessee Valley Authority, with its approximately 70 units in 20 plants and with all the variations of head, load, capacity, etc. for the different projects, affords an interesting variety of typical plant arrangements. With two exceptions the main-river developments employ propeller turbines, usually of the Kaplan type, to meet varying conditions of head and load. Storage developments on the five principal tributaries are provided with moderate head Francis turbine installations, while the so-called secondary storage developments, on streams having relatively limited storage but steep slopes, are the tunnel and surge-tank type, equipped with medium head Francis turbines.

The economics of power plant design is controlled by the specific speed, peripheral coefficient, and critical sigma, i.e., the cavitation limit of the turbine selected. These factors are all interrelated and, in a properly selected turbine, they are compatible. A higher specific speed must not be obtained at the expense of a safe plant sigma value, and a margin of safety of a few feet over the limiting value of the static draft head should always be observed. Furthermore, the turbine should be selected in the basis of its performance under the known operating conditions of the plant.

These basic rules were generally observed in selecting the turbines for the Authority. However, on some of the Francis turbines with heads 90 ft. and above, the sp. speed was reduced to what might be considered relatively low and conservative. In the main-river plants which operate under low heads and varying tailwater elevations, it was necessary, in order to obtain a high enough plant sigma for all conditions of low tailwater, to set the runner below normal tailwater, thus obtaining a negative draft head. This results in the wheel being flooded normally and, in order to gain access to the runner, an unwatering system using pumps was installed. An air system, separate from the station-service system, with a 330 cu. ft./min. compressor operating at 100 lb./sq. in. and with air storage varying from 2000 to 3,500 cu. ft., depending upon the volume of the draft tubes at each plant, is provided. The control diagram for one such system is shown in Fig. 1.

Mechanical Details.

The Authority has adopted the practice of using cast steel as the metal for all heavily stressed parts. The eight original 35,000 h.p. units at one plant are equipped with cast-iron runners, but the six new units, four now in operation and two being installed, are equipped with cast-steel runners. The recent failure of a cast-iron runner which had been in operation in the plant of a utility company for about 12 years, substantiates the wisdom of this policy. Furthermore, cast steel has a much greater resistance to pitting and can be welded in a horizontal, vertical, or overhead position, without requiring pre-heating or stress relieving and without having to be drilled or tapped for studs on close centres as is almost a necessity with cast-iron runners. While bronze is also an excellent metal to resist pitting on turbine runners, pitted areas can only be filled in by a brazing process in the vertical or nearly vertical position, and the entire casting must be pre-heated.

The guide vanes are steel castings, running in bronze bushings with grease lubrication. There is a tendency for the grease to be squeezed out on the loaded side of the bearing, and for corrosion or rusting to occur on these areas. On the high head turbines it was advisable to add a sleeve or bushing shrunk on to the upper and lower guide-vane journals, as well as a stationary bushing in the head cover and discharge ring in which the guide-vane journals rotate. An interesting development is the use of chromium plating by the electrolytic process whereby a deposit of 0.005 in. thickness will be added on to the guide-vane stem and polished to form a corrosion resistant journal. This will probably be adopted on the turbines now being built because of the present war restrictions on stainless steel and bronze. It has been found advisable on the high head turbines to apply a strip of corrosion resistant steel to the top and bottom edges of the guide-vanes where they move adjacent to the stationary parts, and also on the contact edges where adjacent guide-vanes touch each other in the closed position. When high head units are motored for a long period, there is bound to be a slight leakage both at the bottom and top of the guide vanes and where they contact each other in the closed position. This may cause erosion similar to a scouring action. On one 360 ft. head project, a strip of stainless steel about 2 in. wide is being welded on the top and bottom of the guide-vanes and on the tip and on the large end of the guide-vanes where they contact adjacent vanes in the closed position. On another high head project now being built, these areas will be chromium plated to save stainless steel. In the case of the Kaplan and propeller type turbines, it has been found satisfactory to paint these surfaces in order to prevent rapid corrosion of the finished steel.

Scroll cases on the low-head main-river plants are concrete. The high-head storage plants on the tributaries have riveted plate steel scroll cases of the conventional type, except in one station which has cast-steel scroll cases, and in another which will have welded steel scroll cases.

Rolled plate steel throat rings on Kaplan or propeller units are superior in respect of pitting resistance than cast-steel. The Authority's present practice is to specify rolled steel welded type throat rings on all Kaplan and propeller type turbines, but with the restrictions of the use of heavy rolled steel sections, manufacturers have had to change over to cast-steel throat rings on two of the turbines.

The units in the main-river plants all have water lubricated main turbine bearings. Two of these units are equipped with lignum vitæ bearings of the adjustable type, two are of the rubber lined non-adjustable type and the majority are of the Insurok adjustable type. In all cases the Insurok strips are wedged into adjustable shoes which can be adjusted to take up the wear. The

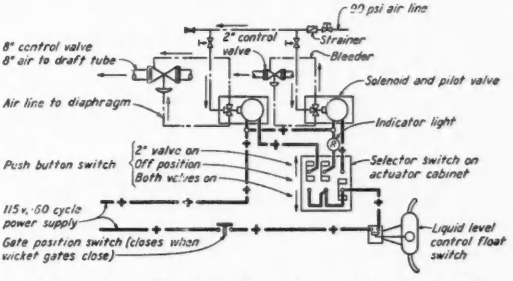

Fig. 1. Control and Wiring Diagram for Draft-Tube Water-Depressing System.

bearing surface on the shaft in all cases is stainless or high chromium steel sleeve. All of the 12 units in the storage or tributary plants have oil lubricated babbitt lined bearings working directly on the polished steel of the main shaft. The lubricating system on all these bearings consists of an a.c. motor driven circulating pump, with a d.c. stand-by motor unit.

All shafts are open hearth carbon or alloy steel forgings, heat treated, and smooth machined finish. They are fitted with renewable sleeves where they pass through the water lubricated guide bearing and the stuffing box in the head cover. All are hollow-bored and given internal inspection to detect any flaws or cracks.

All governing systems are of the relay valve "actuator" type with motor driven governor head, complete auxiliary control mechanisms, restoring mechanisms, oil pressure systems, piping, and, in the case of the Kaplan units, the control valve for runner blade adjustment. Gate opening time, as controlled by the governor varies from a minimum of 4 secs. to a maximum of 12 secs. Speed level controls are set to adjust the speed of the turbine from 85 per cent. of rated speed at no load and zero speed drop to 105 per cent. of rated speed at full load and maximum speed drop. The governing systems are designed for a pressure of from 250 to 300 lbs./sq. in. but tests on units already installed indicate that a pressure of less than 200 lbs./sq. in. is required to operate the wicket gates.

Methods of Preventing Cavitation.

The Authority's experience indicates that pitting can be materially decreased or nearly eliminated, by observing carefully five major points.

1. The turbine runner must be set with proper relation to normal tailwater, and for this purpose careful cavitation tests on a model are desirable.

2. The turbine parts and the water passages must be properly designed.

3. Suitable materials must be used. As just discussed, welded plate steel throat rings offer a great deal more resistance to pitting than cast-steel throat rings.

4. Suitable protection must be provided by the use of stainless steel and other corrosion resistant materials.

5. Operations must be within judicious limits as to capacity and heads, based on the information obtained in the cavitation tests on the model, and from vibration or noise tests on the actual installation.

PRACTICAL TURBINE LUBRICATION

By S. R. O'DETTE. (From *Iron and Steel Engineer*, Vol. 20, No. 4, April, 1943, pp. 34-43.)

THE effectiveness and nature of the lubricant in a turbine may affect not only the continuity of operation but, to an important degree, the operating cost. The following discussion will dwell on the general subjects of turbine lubrication systems and lubricant functions, requirements and maintenance.

Turbine Lubrication Systems.

Piping and General Layout.—There are many large differences in design between large and small and between new and old turbines. Steam pressures are relatively low in the older units, and the construction of these turbines usually is such that lubrication systems can be readily dismantled for cleaning. Such simplicity of construction is often employed on small modern units, but not on the larger high-pressure, high-temperature turbines. Further complications arose with the advent of high-pressure, high-temperature steam. A serious hazard was that of fires caused by oil line breakage or leaks. To eliminate this danger, early consideration was given to the possibility of non-inflammable lubricants. The hazard was finally reduced greatly, however, by removing or shielding high-pressure oil lines from hot steam lines and valves. The unavoidable result was greater complication in the lubricating system.

Many machines installed to-day take steam at high pressures and temperatures, and exhaust at lower pressures, to older or lower pressure turbines. They also bleed off steam at various temperatures to operate other equipment or to supply other needs within the plant. All of these functions are controlled by automatic apparatus which use the oil from the lubrication system as a hydraulic medium. Not only is this a further complication, but the extremely fine clearances in such control mechanisms place new requirements of stability on the lubricant. Any necessity, therefore, to dismantle such modern systems for cleaning, due to oil failure or degradation, is not only prohibitive from a machine-down time and cost standpoint, but there is little possibility of removing all deposits from parts and oil passages.

Reservoirs.—In the older turbines the oil reservoir is usually cast iron and is an integral part of the turbine construction. In the newer machines the use of cast iron in the construction of oil reservoirs is confined almost entirely to small auxiliary units. Reservoirs for the larger turbines are fabricated from steel plates and placed in such a position that they are more accessible for inspection. Because of the importance of cleanliness of the lubricant, the trend is to construct these reservoirs with sloping bottoms. Many of the flat-bottomed oil reservoirs have their drain-off connection several inches above the bottom of the tank. These reservoirs have been improved materially by adding a water leg to the bottom of the sump as a means of effectively collecting the water and solids. In some other cases a bell-bottomed suction pipe from the purifying system can be placed directly on the bottom of the sump.

In some of the later designs the shallow, broad oil reservoir is giving way to the tall, narrow reservoir. One advantage is that the area of exposed metal above the oil level, subject to rusting, is reduced. A further advantage is that, due to the lower oil velocity near the bottom, tall tanks permit precipitation of water and solids more readily than do the shallow tanks where the oil flow is maintained at a more uniform velocity.

Oil Cooler Placement.—Because of space limitation and structural designs, the coolers are often found below the lowest point of the lubricating system, thus providing a place for deposits to collect. Since such formations are particularly undesirable in or on cooler tubes, the ideal situation is to place oil coolers in a vertical position at least on a level with the oil reservoir and certainly not below it. Cleaning of the oil side of lubricating oil coolers can be completely eliminated by careful selection of the lubricant and efficient operation of oil maintenance apparatus, coupled with correct oil cooler placement.

Turning Gear Operation.—When a high-pressure turbine is being shut down it may require at least 24 hours in turning gear to reduce the rotor and casing temperature to about 250° F. where the machine can

be stopped without fear of distortion. During this time difficulties can be encountered in bearing lubrication, due to the difficulty in maintaining oil films at low journal speeds. Investigations have shown that bearing failures during starting or stopping were due to a tar-like mass of deposit which formed between the bearing and the journal and prevented the possibility of establishing a fluid film. The viscosity of the oil should be as high as possible while the machine is in turning gear. A number of turbine builders recommend, therefore, that when a machine is to be taken off the line and placed on turning gear the oil coolers should be opened wide in order to reduce the temperature and increase the viscosity of the oil as rapidly as possible.

Turbine Oil Functions.

Lubrication.—Turbines have rarely been built with insufficient bearing area to support the loads. In general, turbine bearings are almost the ideal case for fluid film lubrication. Loads may range from 20 to 200 lb./sq. in. with 50 to 150 the average. Speeds of the journal fall in the neighbourhood of 150 to 175 ft./s. and radial clearances average 0.002 in. per in. diameter. Because of the high speeds in the turbine spindle, there is an adequate pumping action of the journal itself, which carries oil into the bearing area in sufficient quantities to float the spindle on the oil. The high rotational speeds and the large amount of heat conducted to the journal from the steam in the turbine itself make it imperative, however, that the oil film should not fail, as even slight interruptions in the fluid film may be sufficient to score surfaces or overheat the metal. Viscosity requirements vary, depending upon the speed of the turbine, the method of lubrication, and whether or not reduction gearing is lubricated simultaneously. In other respects, however, the strictly lubricational requirements of a turbine oil are relatively simple.

Cooling.—The major portion of the oil circulated acts as a coolant. Accurate observations indicate that the oil actually lubricating the turbine spindle may leave the pressure area at a temperature near 250° F. Since the relative volume of oil actually supporting the bearing spindle is about 10% of the total volume fed to the bearing, the mean oil temperature leaving the bearing is always much below this figure.

Hydraulic Medium.—Modern turbines incorporate exceedingly complex mechanisms to give the precise control and automatic operation now expected of all prime movers. Almost all such devices depend, at least in part, on hydraulic service and control units utilizing the turbine lubricant as the hydraulic medium. The critical nature and close tolerances of such devices impose new requirements of stability and cleanliness on the lubricant, far exceeding those considered outstanding even a few years ago.

Surface Protection.—Since some water can always be anticipated within a lubricating system, and since even minute quantities of water will promote corrosion of ferrous metal surfaces, it is necessary that the lubricant should effectively " wet " all surfaces bathed by the oil, to prevent the water from coming in direct contact with the surfaces. This protection must be accomplished without impairing heat transfer.

Quality Requirements.

Acidity.—All turbine oils are practically neutral when new. In use they develop a slight amount of acidity which, in modern oxidation inhibited turbine oil, does not increase rapidly until near the end of the useful life of the particular batch of oil. If acidity is excessive it may gradually attack the metal of the turbine system and form metallic soaps. The soaps, if highly concentrated, may also precipitate to add to the sludge deposits formed in the system. However, while the acid content of an oil may even discolour metal parts, real damage due to corrosive action from this source alone is doubtful. Acidity is of principal interest as an index of the rate of oil deterioration due to oxidation.

Oxidation.

Oxidation.—Important to the turbine operators is the fact that the rate of oil deterioration can now, in most cases, be reduced to an almost negligible amount over long periods of time by selection of a modern correctly-finished turbine oil, intelligent design and operation of the turbine, and by adequate oil maintenance. Oxidation may take several forms. The results are increases in viscosity, development of acidity, sludge formation, or other effects. Some oxidation products form deposits, either solid or lacquerlike, or may cause corrosion.

Resistance to Water.—Moisture is the most common contaminant tending to prevent turbine oil from functioning satisfactorily. Water may enter through leaky glands, cooling coil leaks, sweating at the pipe connections, etc. Although pure water alone is not injurious to clean oil, it must be removed promptly, since large quantities may float the lubricant above the oil pump suction. There are numerous operating difficulties which may be traced to moisture in the system, or which may be aggravated by the presence of moisture. Turbine oils must have the highest possible resistance to emulsification with water. For practical purposes, turbine oil emulsions can be considered as a mixture of oil, water and solids, and air. These substances can be combined mechanically in such a manner that they are held in suspension. While common emulsions in themselves are not always harmful, they do not make good turbine lubricants, and, when pumped through the system, may cause real harm. In passing through the close clearances in the system, the pressures and temperatures tend to break the emulsion. This causes the solids present to precipitate and adhere to these areas, forming hard deposits. Under aggravated conditions, the solids built up in the bearings by this action may totally disrupt fluid film lubrication.

Surface Protection.—The lubricant obviously must not be injurious, under any condition reached in service, to the materials of the lubrication system. Difficulties of such nature are rare to-day.

Protection Against Water Corrosion.—Excessive water or moisture within the oil system may cause serious corrosion, particularly in the areas which are not bathed with oil. Moisture condenses on these surfaces and, as it drops into the lubricant, it carries with it finely-divided particles of rust. Moisture corrosion can develop even on surfaces bathed with oil, due to inability of the oil to displace deposited moisture. Particular emphasis is placed upon the moisture corrosion which can occur when starting new turbines. Moisture then carried in the oil will cause serious corrosion unless the lubricant has sufficient metal-wetting ability to prevent the free moisture from coming into contact with the fresh metal surfaces. Modern chemistry has provided a practical solution by adding wetting agents to a new turbine oil. In many cases where the products of corrosion have been a problem, real improvement has been made by fitting or equipping many large turbines with bag filters, centrifuges, wash towers, or combination of these, so as to remove such corrosion products promptly. Much attention has been focussed also on coatings that might be applied to the interior surfaces of the lubricating system. The coatings must last a very long time, and it also must be impervious to both oil and water at elevated temperatures. A long search has shown that at least one coating, using a synthetic vehicle pigmented with finely-divided pure aluminium meets all service requirements.

Turbine Oil Maintenance.

Proper equipment for turbine oil maintenance is highly desirable in any turbine installation. Equipment commonly used for oil maintenance includes centrifuges, bag filters, oil conditioners, blotter presses, asbestos filters, rest tanks and combinations of these. In the operation of any of this equipment there is a definite need for the turbine operator to filter the oil at higher oil temperatures than he might normally select. Practical experience has shown that it is almost impossible to remove finely-divided solids and moisture from turbine oil when filtered at above 130° F. To-day engineers are recommending periodic centrifuging at 150° F. or even 180° F., with excellent results. It will be found that centrifuges will evaporate finely-divided solids and water much more efficiently if, in addition to raising the oil temperature, the rate of oil passing through the unit is decreased considerably. Excellent results are obtained by operating at 50% and even 25% of the rated capacity of the centrifuge. It is often desirable to add hot water to the lubricant going to the centrifuge. One reason is that some of the products of oil oxidation are water soluble and are thereby dissolved and washed from the lubricant. Hot water performs another function on finely-divided products; when wetted, these particles coagulate or coalesce, forming particles of such magnitude that they can be more readily extracted in the centrifuge.

The conventional bag filter is capable of removing water and finely-divided solids if the rate of the oil passing through the unit is sufficiently low so that high turbulence is not encountered. The failure of many filters of this type to maintain oil in the best possible condition can usually be traced to operating the filter at too low temperatures and at such large flow rates that the finest particles are literally forced through the cloth filter. The addition of hot condensate with the lubricant in the precipitation compartment prior to passing through the bag filter is rapidly gaining favour for the same reason that it proves effective in centrifuging. Blotter presses have proved quite satisfactory for the removal of small quantities of moisture and finely-divided solids entrained in the oil. Difficulty in the use of such equipment occurs, however, when the oil supply for the blotter press is taken from a connection on a high-pressure oil line.

Another type of mechanical filter finding great favour among turbine operators is one fitted with asbestos wafers of varying density. The reduction in solid particle size is readily accomplished by the selection of the correct wafer density.

On all the types of oil maintenance apparatus which have been discussed above, it should be noted that the efficiency of the cleaning operation is greatly increased by drawing the oil from the intermediate bottom of the oil reservoir.

DIRECT PNEUMATIC HAMMER RIVETING in AIRCRAFT PRODUCTION

By Ing. F. Wilde, VDI. (From *Maschienenbau, Der Betrieb*, Vol. 21, No. 8, August, 1942, pp. 337-340.)

When light metal aircraft structures were first riveted with the pneumatic hammer it was attempted to adopt the method of "direct" riveting known in boiler and bridge building. To carry out riveting according to this method a holding-on tool (*b* in Fig. 1) is pressed against the die head, and the pneumatic hammer (*a* in Fig. 1) drives the closing head by upsetting the rivet shank. Due to inaccessibility of the rivets the driven head was often damaged at that time. This was overcome by applying the forming tool to the die head (*a* in Fig. 2) and driving the rivet by the holding-on tool (*b* in Fig. 2) on the closing head side. This method is termed as "indirect riveting," and it is in general use with pneumatic hammers. The assumption hereby is that the energy necessary to form the closing head is afforded by the mass of the holding-on tool. However, this becomes impossible with bulky components, which absorb so much of the work that the excess energy is insufficient for forming the closing head. Thus it appears to be necessary to revert to direct riveting. Direct riveting becomes necessary at a length of rivet shank of over 30 mm. with light metal, and of over 20 mm. with steel.

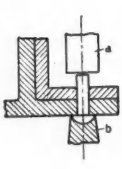

Fig. 1

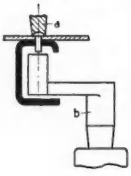

Fig. 2

Pneumatic Hammers.

In principle, for driving the rivets, the customary tools developed for light metal work can be used for direct riveting too. The high-speed hammers used generally for indirect riveting (3,000 to 4,000 blows per minute) demand, however, great skill from the workman. Satisfactory heading is difficult to achieve; the conditions are more favourable in this case with steel parts, as the hot-driven steel rivet does not require a great number of blows.

More suitable for the purpose are, therefore, low-speed hammers (750 to 1,500 blows per minute) with a greater piston stroke, giving greater energy per blow. (See Fig. 3: the two upper tools by Ipeg, Berlin, the lower hammer by Frankfurter Maschienenbau A.G.,

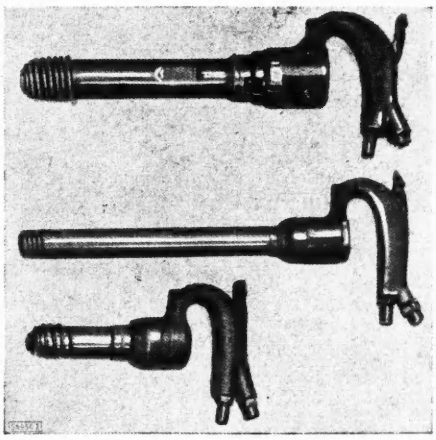

Fig. 3

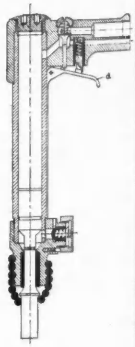

Fig. 4

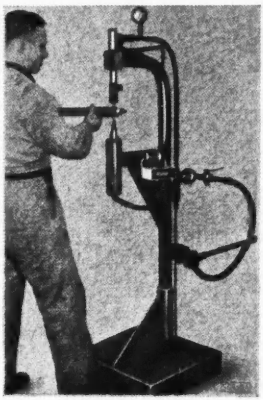

Fig. 5

Frankfurt a. Main). But even these hammers developed as they are for aircraft work, are not equally suitable for every type of work. Special hammers have been developed, therefore, for direct riveting. These execute single blows with a great energy, imitating thus to a certain extent the process of hand riveting. Fig. 4 shows such a tool, built by Ipeg, Berlin. The hand lever "*a*" actuates the hammer. This is a peculiarity of all German single-blow hammers, while with French and American types the hammer blow is achieved by pressing the tool on to the rivet. Generally three to five blows are required to drive a rivet.

The single-blow hammer mounted in a stand or frame has found extensive use as a stationary tool. (See Fig. 5, maker : Ipeg, Berlin.)

Holding-on Tools.

As it is desirable to rivet light metals in a cold state the work required for upsetting the rivet shank when closing the rivet is considerably greater than that for

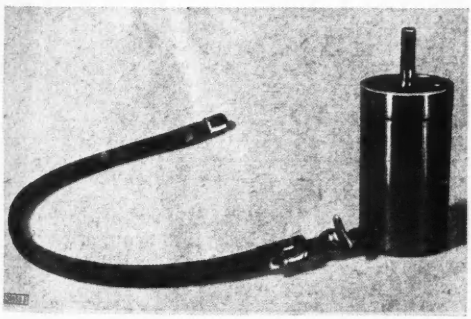

Fig. 6

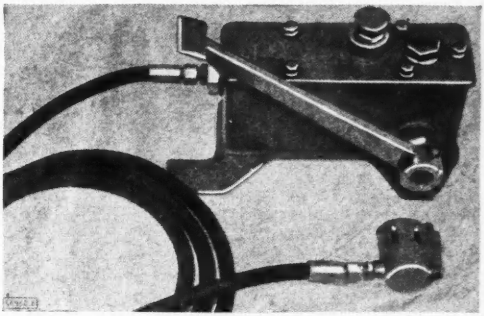

Fig. 7

hot-driven steel rivets ; the mass of the holding-on tool must be greater accordingly. It is recommended, wherever possible, to use a holding-on tool such as shown in Fig. 6 (compressed-air piston) supported against the structural part, for duralumin rivets with a shank diameter over 4mm. The piston area is to be chosen so as to produce 600 kg. holding-on load per each cm^2. of shank cross-sectional area. For steel rivets the required pressure is only 50 kg./cm^2.

In many cases it will be impossible to provide a big enough piston to produce the pressure necessary for satisfactory riveting. The remedy lies with hydraulic holding-on devices such as shown in Fig. 7, which is operated by three to four strokes on the pedal. The pressure in the piping is about 150 kg./cm^2.

Another solution, for emergency cases only, is to use a second pneumatic hammer as holding-on tool.

Application.

In the foregoing the range of applicability to direct riveting has been outlined. From a study of the time of riveting it becomes obvious that even before reaching the limit of applicability of indirect riveting, the direct riveting can be of advantage. Fig. 8 shows that the intersection of the two respective curves is at about two-thirds of the limit of indirect riveting.

Summing up it can be stated that riveting with pneumatic hammer can be applied where the use of riveting presses is impossible.

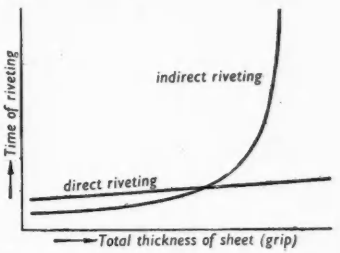

Fig. 8

THE INFLUENCE OF RIVETING TOOLS ON THE DRIVING OF HEAT-TREATED LIGHT METAL RIVETS

By Emil von Rajakovics and Adolf Teubler, Berlin-Borsigwalde. Report of the Research Institute of the Durener Metallwerke A.G., Berlin. (From *Werkstatt und Betrieb*, Vol. 75, No. 8, August, 1942, pp. 189-191.)

The rivet material considered here is "Duralumin LN93," a special rivet alloy of the Al-Cu-Mg variety according to DIN1713, which was developed three years ago by the Durener Metallwerke. Rivets of this alloy are heat-treated to 500° C., quenched in cold water, and driven within a relatively short time, the so-called "ageing" period. This period, during which the rivet can be satisfactorily driven without danger of cracking at the closing head, is dependent on the ageing temperature. Throughout this report the

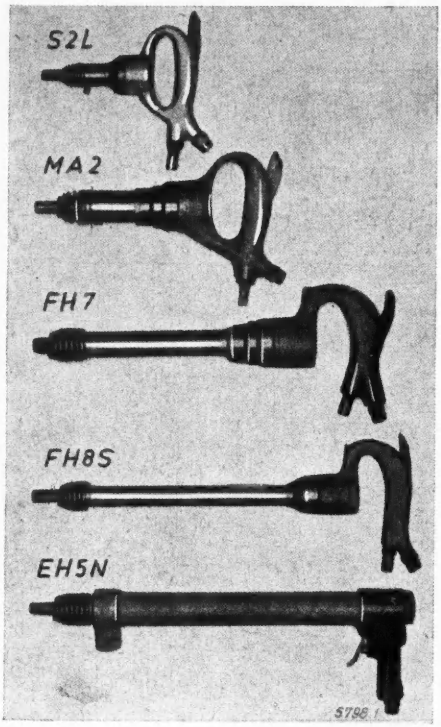

Fig. 1

ageing temperature is taken to be 20° C, and that state of formability of the rivet shank by upsetting without cracking alluded to above, will be called "plasticity." The riveting tools used were a pneumatic riveting press of the type SDM326, and five various pneumatic hammers (Fig. 1) to cover the low and high-speed range. (Tool E H 5 N is identical to that shown in the sectional view in Fig. 4 of the preceding article on p. 196 ; FH7 and FH8 can be identified as the two upper tools in Fig. 3 on p. 196.—Editor, *E.D.*) The more important data of the tools shown in Fig. 1 are contained in Table I.

TABLE I.

Type	Suited for duralumin flat head rivet up to . . . mmϕ	Suited for duralumin brazier head rivet DIN L71 up to . . . mmϕ	Length of tool mm.	Weight kg.	Number of blows per minute
S2L	4	3	156	0.9	3,700
MA2	6	5	230	3.3	2,700
FH7	8	6	385	4	1,200
FH8S	7	5	420	2.8	800
EH5N	4	3	420	3.6	single blow hammer

The extremely low weight of the tool S2L is due to its light metal handle. Riveting by hand has not been included in the comparison because experiments have shown that to drive rivets by hand-hammer 5 to 15 times as much time again is required than with the riveting press. The diameter of the rivet shanks used in the test was 4 and 6 mm. The shape of the rivet head and other conditions of the tests are tabulated in Table II.

TABLE II.

Rivet diameter mm.	Riveting tool and type	Shape of head according to	Shank excess length for heading mm.	Type of riveting
4	Riveting press SDM326	RDLI *	6	Direct riveting
		DIN9011	5	
	Hammer S2L	„ †	5	Indirect riveting
	„ EH5N	„	5	
	„ FH8S	„	5	
6	Riveting press SDM326	RDLI	9	Direct riveting
		DIN9011	7	
	Hammer MA2	RDLI	9	Indirect riveting
		DIN3011	7	
	„ FH8S	RDLI	9	
		DIN9011	7	
	„ FH7	RDLI	9	
		DIN9011	7	

As a measure of plasticity, a "plasticity limit" has been defined as that smallest height of head or greatest head diameter with which satisfactory riveting without cracking can be achieved. From this, one can derive the excess plasticity E as the ratio of

$$\frac{100\ H_s - H}{H_s}\ \% = E = \frac{D - D_s}{D_s}\ \%$$

Hereby, H_s and D_s are the depth and diameter of head according to DIN or RDLI standards, and H and D the smallest depth and greatest diameter of head respectively which can be considered just satisfactory.

The test results are plotted in Figs. 2 to 4. Fig. 2 shows the influence of the riveting tool on the excess plasticity E, for rivets of 4 mm. shank diameter of "Duralumin LN93." Fig. 3 contains the same type of data for 6 mm. shank diameter rivets of the same material. Fig. 4 show the influence of the excess

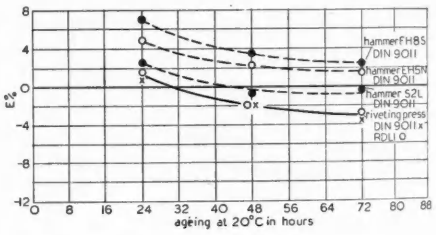

Fig. 2

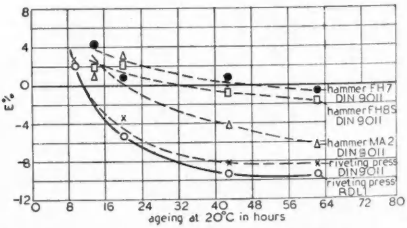

Fig. 3

† DIN = Deutsche Industrie Normen, the equivalent of the British Standard Association.

* RDLI = Reichsverband der Deutschen Luffahrtindustrie, the equivalent of the Society of British Aircraft Constructors.—(Editor, *E.D.*)

shank length for heading on the excess plasticity E for 6 mm. shank diameter rivets of "Duralumin LN93" when driven by low-speed tools. In accordance with Table II the shank excess length is 7 mm. for the DIN9011 rivets (dotted curves in Fig. 4), and 9 mm. for the RDLI rivets (full lines). The curve for tool MA2 has been omitted as with this tool E was equal for both shank excess lengths. Additional data showing the influence of ageing on the Vickers hardness and shear strength are given in Fig. 5.

In conclusion it can be pointed out that the driver head according to DIN9011 is not only easier to form but, being brazier head, it represents considerable weight saving with larger sizes as compared with the older RDLI specification. This is especially true when low-speed tools are employed.

Low-speed tools have proved to be superior to the riveting press also when the driven head was spherical, according to DINL71 specification.

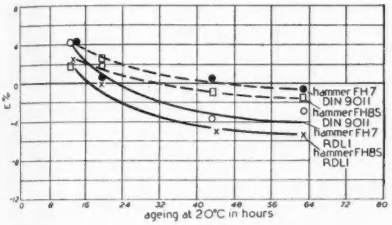

Fig. 4

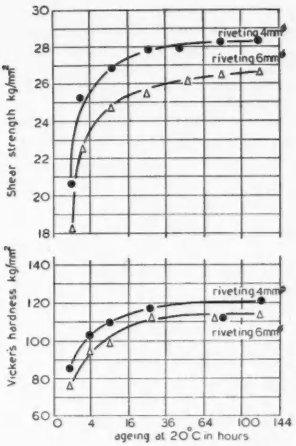

Fig. 5

THE INFLUENCE of REYNOLDS NUMBER at HIGH MACH NUMBERS

By ANTONIO FERRI. (From "*Atti di Guidonia*," Vol. 1942, No. 67-69, 10th March, 1942, pp. 49-92.)

To investigate the influence of Reynolds number near sonic speed, measurements have been made in the Guidonia high-speed tunnel on three spheres of brass of 40, 60 and 80 mm. diameter with rear faired supports, and on two steel cylinders of 15 and 30mm. diameter across the partly free jet. The measurements covered drag, and pressure differences between front stagnation point and a rear point. By means of similar models, which could be turned and had several pressure holes, the pressure distribution around the bodies has been determined.

At Mach numbers up to 0.67 the drag was decreasing with increasing Reynolds number to a minimum value, to rise again slightly with further increase in Reynolds number (Fig. 3). With increasing Mach number the

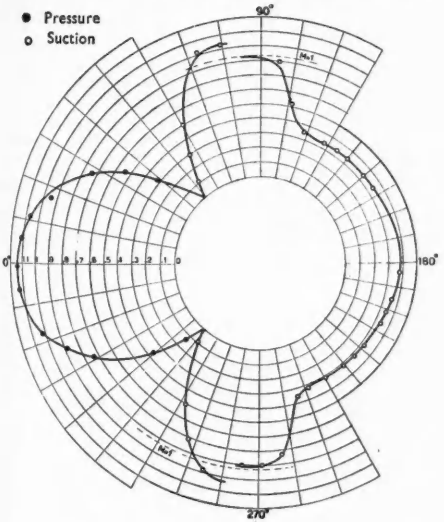

Fig. 1 Pressure distribution around sphere at R = 720,000 and M = 0.70. The dotted circular line indicates that locally the speed of sound is reached (M = 1) and a shock wave occurred.

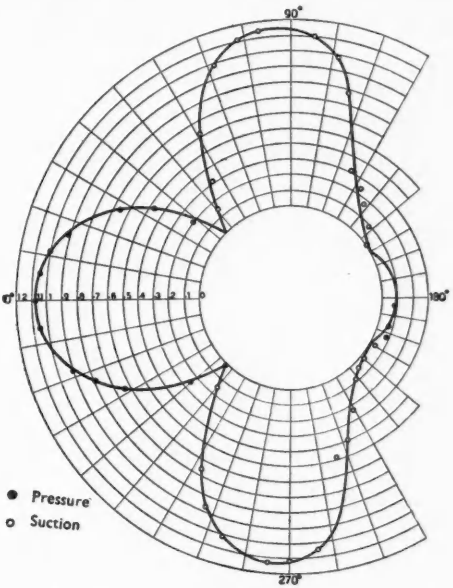

Fig. 2 Pressure distribution at the high Reynolds number 640,000, and the low Mach number 0.55 The stagnation pressure is smaller, the suction on the sides greater, the points of static pressure lie more forward than in Fig. 1. On the lee side, there is a second region of positive pressure.

drag increases, and so does the Reynolds number at which the drag has its minimum value. This is confirmed by the pressure distribution (Fig. 1) as well as by photographs taken by the Schlieren method. With increasing Mach number the positive pressure in front increases; the maximum pressure at the stagnation point is in accordance with the theory, i.e., the dynamic pressure multiplied by $(1+\frac{1}{4}M^2)$. At the same time, the points of static pressure move backward. The rear pressure drop is small with high Mach numbers.

If at Mach numbers somewhat below 0.8, the speed of sound is locally exceeded, shock waves occur at these positions, and the suction in the rear increases. The critical Reynolds number R*cr* is of significance at small Mach numbers only; if R*cr* is exceeded, there is in the rear a second zone of positive pressure (Fig. 2). In this the behaviour of the cylinder is identical to that of the sphere. At supersonic speeds M=1.85 and M=2.13 the Reynolds number has no influence at all; with the increase of drag coefficient the points of static pressure lie almost at 90° and 270°. The rapid pressure drop in the suction zone corresponds to the increased curvature of the streamlines similarly to thin aerofoils near sonic speed. Here the sphere is not suitable any more as an indicator of turbulence. However, with aerofoils the transition from laminar to turbulent flow aft of the first shock wave is dependent on the thickness of the boundary layer, and thus on the Reynolds number.

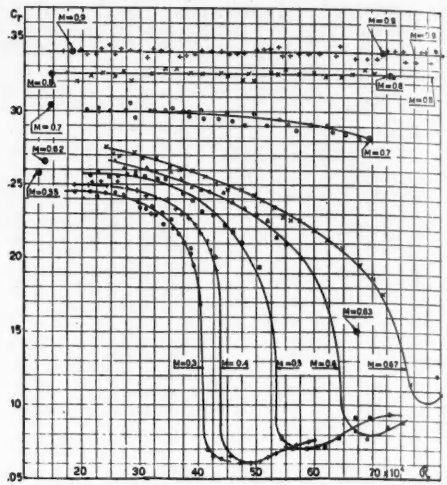

Fig. 3 Drag coefficient of sphere plotted against Reynolds number for various Mach numbers.

FREEZING OF ACIDS IN ACCUMULATORS

By Dr. Ing. Emil Blaich. (From *ATZ Zeitschrift*, Vol. 45, No. 23, December, 1942, pp. 641-645).

During the present war, on both the eastern and the western fronts, vehicles of every description had to be stored for long periods in open places. As the temperature in winter was —40° to —50°C. the acid in the accumulator was found frozen in many instances. The condition necessary for this freezing to occur is, apart from the low temperature, that the battery should be in a discharged condition. In the technical literature there is only one reference to freezing of acids in accumulators in which it is stated that freezing has no ill effects on a charged battery, but might damage the plates if it is discharged. In the present article this problem is more closely investigated.

When does the Acid Freeze?

Within the practical limits of acid (sulphoric) concentration in accumulators of sp. gr. of 1.1 to 1.3, the freezing temperature decreases with increasing concentration, as shown in Fig. 1. It follows, therefore, that a charged accumulator (sp. gr. 1,285) will not freeze in practice. On the other hand, the freezing temperature of a Bosch battery is only about 14°C., corresponding to the acid concentration of 1.16. The concentration might decrease still further if the discharged battery is left unattended for a longer period of time. The rate of self-discharging depends greatly upon the atmospheric temperature and falls off rapidly as the temperature decreases. Another frequent source of trouble is, of course, that during the rest period some leakage of current occurs, when the battery will be discharged very quickly.

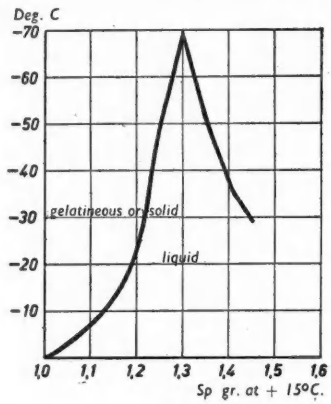

Fig. 1

Bursting effect of Frozen Acids.

It is erroneous to assume, as is normally done, that the acid will burst the glass or other container when it freezes similarly to freezing water. Simple tests can prove that this is not the case with acids. Test tubes were filled with acids of different concentration as shown in Fig. 2, and were exposed to —40°C. for 30 hours. Corresponding to Fig. 1 the acid of 1.25 concentration should not freeze while acids of a concentration of 1.20 or lower must freeze. Fig. 2 shows clearly that this is the case, and also that neither of the test tubes cracked during the test.

That frozen acids have no bursting effect follows from the fact that unlike water acids do not solidify when freezing but remain still "plastic." The state of plasticity depends upon the acid concentration. It was found that the acid of 1.20 concentration could still be stirred, while the acid of 1.02 concentration was sufficiently solidified so that a thermometer could not be inserted.

If, nevertheless, more accumulators are found to burst in cold weather, then this is due to various other reasons. The main reason is probably the increasing brittleness of the accumulator material with decreasing temperature. This is shown in Fig. 3. Accumulator cases were cooled to different temperatures and then dropped under identical conditions. The height from which the cases were dropped was gradually increased

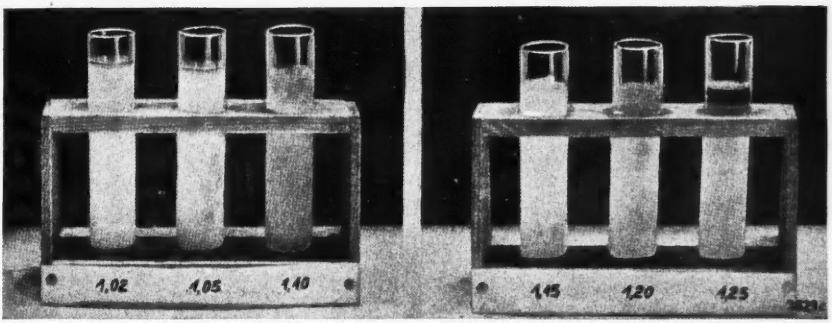

Fig. 2

until they broke. Another reason for frequent breaking of accumulators in cold weather is due to rough handling, probably aggravated by handling them with frozen, stiff hands.

It could also be argued that the accumulator case might burst if distilled water is added to the still frozen acid. This assumption, too, fails when tested. The reason for this is that the heat content of the water added is sufficient to melt a very small quantity of the acid which will mix with the water and this is sufficient to raise the concentration of the newly formed mixture so that no bursting occurs.

Discharging of Accumulators with "Frozen" Acid

The internal resistance of a battery increases as the temperature decreases, and jumps to a high value when the acid freezes. As a consequence the voltage across the terminals is also much reduced, as can be seen in Fig. 3. The curves were obtained by measuring the voltage about 2 secs after connection to ensure stable conditions. The decrease in voltage between +20 and —40 °C. is the result of higher viscosity due to cooling, while the much higher difference between the fully charged and only half full battery at —40° is a sign of freezing. The full battery does not freeze at —40°, while the half-full battery freezes as can be seen in Fig. 1.

Starting up an engine with a frozen battery is not possible for two reasons. The first is the low voltage across the terminals which is insufficient for the required speed of the motor, and the second reason is that freezing affects the battery capacity so that it is rapidly exhausted.

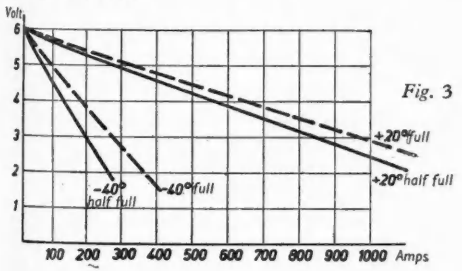

Fig. 3

In Fig. 4 the current supply from a 6—V, 75 —Ah battery is shown at —40°, when full and half full. A similar battery would deliver at +20°C. about 85 Ah, when full and about 43 Ah when half full. As can be seen from the figure at —40°C. these figures are much reduced. The full battery delivers only about 37% of that obtainable at +20°C., while for the half-full value the corresponding figure is only 15%. Although under such conditions the battery can still operate the ignition

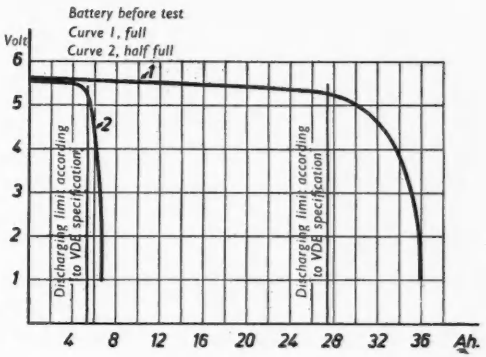

Fig. 4

system of the engine, it would fail for starting or other purposes.

That heating of the battery increases the electric supply obtainable from a frozen battery, without recharging, is shown in Fig. 5. From a 75 Ah battery 40 Ah were first taken at +20°C. Subsequently it was cooled to —42°C. when the acid froze and the battery was completely exhausted. On reheating to +20°C. further 14 Ah could be taken from the same battery without changing. The figure also shows a similar curve for temperatures of +20°, —30°, +20°C.

To investigate whether the capacity of batteries is affected by freezing, two batteries were kept at —40°C. for 10 days. Two other batteries were exposed to temperature variations between —40° and +20°C. each cycle lasting for 48 hours. The following table gives the capacities of these batteries before and after cooling.

TABLE I.

	Capacity in Ah.	
	Before Freezing	After Freezing
For ten days to —40°C. ..	69 68	75 74, 5
20 temperature changes between —40° and +20° ..	69 70	74, 5 74
Standard battery kept at +20°	69	76

The Table shows that in no case was the capacity reduced by heating, but actually there was an increase

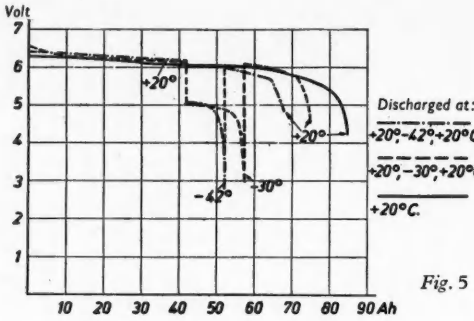

Fig. 5

in capacity. This is probably due to the fact that the batteries were new and in this stage the plates were not completely formed.

Charging of Batteries with Frozen Acids.

In a previous article on this subject it was pointed out that the charging voltage of a frozen battery is considerably higher than that under normal conditions. This is to be expected since the internal resistance increases due to freezing. A frozen battery must not be charged, since the acid is forced out from the battery in the form of froth, but it soon liquifies outside. It is interesting that for varying charging current and temperatures the same A. hrs. must be supplied to the battery before froth appears outside the battery. This might be explained by the fact that the charging current produces no chemical changes but only decomposes water. The quantity of gas produced in this way is, of course, proportional to the current. The gases cannot escape through the frozen acids, but forces the acid level up. Charging of frozen batteries is therefore not permissible for two reasons: (a) the overflowing acids destroy all metallic materials with which they come into contact, and (b) the gases produced are responsible for high internal pressure which might lead to bursting of thin battery containers.

DESIGN OF D.C. MAGNETS

By L. T. RADER, Associate A.I.E.E. (From *Electrical Engineering*, Transactions, Vol. 62, No. 6, June, 1943, pp. 307-310.)

D.C. MAGNET design is of tremendous importance to-day because of the almost exclusive use of D.C. power in mobile equipment, such as tanks and airplanes. Magnets are the backbone of the D.C. control systems, for, when energized by push buttons or interlocks, they furnish the power to operate contactors and relays of all descriptions or to perform mechanical functions, such as actuating firing pins or locking devices. Such applications require light weight, minimum volume, insensitivity to vibration with the magnet open or closed, higher operating temperatures, etc.

The diversity of design requirements has led to a large number of different forms of magnets. It is impossible to find a design procedure suitable for all cases, but the same factors, such as saturation, leakage, residual forces, and kind of steel, must be considered in each.

Tables I. and II. list the magnetic properties of
Cold rolled or stamping steel,
Silicon steel,
Low metalloid steel or ingot iron, and
High-saturation steel such as 50% cobalt, 50% iron.

Ageing factor (Table I.) is defined as the per cent. increase in hysteresis loss which occurs to a steel with time. As applied to D.C. Magnet design, an increase

TABLE I. MAGNETIC PROPERTIES OF D.C. MAGNET STEELS

Kind of Steel	Alloying Constituent (Per Cent.)	Intrinsic Saturation (Kilolines Per Square Inch)	Ageing Factor (Per Cent.)	Residual Induction (Kilo-gausses)	Coercive Force (Oersteds)	External Energy (Maximum)
Common ..	0.25 silicon maximum ..	133	15	7.9	1.5	4,650
Silicon *A* ..	0.25–0.75 silicon ..	132.3	8	8.37	0.86	3,450
Silicon *B* ..	0.75–1.25 silicon ..	131.5	5	8.0	0.70	2,400
Silicon *C* ..	2.50–3.0 silicon	126	3	8.1	0.67	2,450
Ingot iron ..	None	135.5	Varies	7.5	1.05	2,330
Cobalt	50 cobalt	148	—	16.5	3.5	25,800

TABLE II. MAGNETIZATION DATA FOR D.C. MAGNET STEELS

Kind of Steel	Total Flux Density (Kilolines Per Square Inch)												
	10	30	50	70	80	85	90	95	100	105	110	115	120
	Magnetizing Force (Ampere Turns Per Inch)												
Common ..	1.98	3.55	5.1	8.1	11.1	14.1	19.2	28	45	77	136	235	355
Silicon *A* ..	1.17	2.05	3.35	6.2	10.3	14.8	22.5	38	66	120	192	290	420
Silicon *B* ..	1.20	2.05	3.3	6.4	10.9	15.0	22.5	39	69	120	195	300	430
Silicon *C* ..	1.10	1.79	3.1	6.4	11.8	18.5	34	65	116	187	280	410	570
Ingot iron ..	1.2	2.3	3.5	5.2	6.6	7.5	8.9	12.0	21.5	55	115	165	257
Cobalt	2.6	4.4	5.3	6.0	6.3	6.6	6.9	7.4	8.1	9.0	10.5	12.5	15.8

in the hysteresis-loop area is significant principally in the second quadrant, where an increased area means an increase in external energy and in coercive force. An accepted laboratory method of finding the ageing factor is to measure the D.C. hysteresis loop before and after holding the steel at 100°C. for 600 hours.

Cold rolled steel is the most widely used for D.C. magnets because of its low cost, and its desirable mechanical qualities. It is readily drawn, punched, or formed, and is available in many forms and sizes. As, however, the mills do not guarantee its magnetic qualities, large variations can and do occur in the magnetic quality of this steel. In general, in the annealed condition, it has a better magnetization curve for the higher densities and a higher saturation value than the silicon steels. Its coercive force and its available external energy are high, and its ageing factor is large. A design using this material must be checked carefully, not only for residual forces at the time of manufacture, but also for increased forces which may develop because of ageing.

As the percentage of silicon in steel increases, the saturation curve becomes poorer, and the intrinsic saturation falls. Silicon steels are also harder to fabricate. Silicon steels, however, are sold with specified magnetic properties and are of consistent quality. Ageing factor, coercive force and external energy are considerably less for silicon steel than for cold rolled steel.

Ingot iron is the purest form of iron sold commercially. When properly annealed, it has the best magnetization curve and the highest intrinsic saturation value of the usual steels. It is ductile and tough, but readily forged, machined, or welded. Its external energy curve is low. Its main disadvantages are its relatively high cost and lack of availability in various forms and sizes.

Special high-saturation steels are relatively difficult to obtain, they are expensive, have poor machining properties, and high coercive force and residual induction. However, a 50% cobalt, 50% iron has a remarkably good induction curve and high intrinsic saturation.

In all D.C. designs, especially in those using cold rolled steel, it is essential for consistent performance that an air gap be in the circuit between the armature and pole face. The order of magnitude of residual forces is often underestimated. In one case a magnetic circuit of ingot iron weighing 5 lbs. 2 ozs. was found to have 33 lbs. residual force when there was no air gap in the circuit. In another case a small relay using annealed stamping steel weighing 32 grams had a measured residual force of 112 grams. When a magnet operates, the repetitive shock of one part on another, together with the simultaneous application of magnetic field, tends to increase the coercive force. It has been found in practice that this increase may be considerably more than the ageing factor would indicate.

D.C. magnets can be classified into two general groups :

1. Clapper or pivoted armature type.
2. Solenoid or pot type.

Fig. 1A shows a typical form of clapper magnet. An armature is pivoted on one face of a U-shaped piece, and rotates through an air-gap to strike a pole face. The coil may be placed on any leg of the core. Fig. 1B shows a solenoid-type magnet in which a plunger, usually circular, moves within a coil to strike a core or head finally.

Design requirements for a magnet are usually :—

1. It should give a force-versus-stroke curve suitable for the particular requirement.
2. It should utilize to the fullest extent every ounce of iron and copper in the magnet.
3. It always should release under the action of the restoring spring when de-energized.

These requirements determine whether a clapper or solenoid magnet will be used. The shape of the pull curve of a clapper magnet can be changed by varying the pole-face area ; that of a solenoid type by using some variation of a stepped plunger or conical plunger.

In order to find the flux in a circuit consisting of an iron path in series with a short air gap, a trial-and-error method is usually employed. A value of flux is assumed ; the various megnetomotive-force drops are found, and their total compared to the applied magnetomotive force. A result sufficiently accurate can be obtained usually in two or three trials. When the flux is found, the force between faces is obtained from

$$F = \frac{B^2 A}{8\pi} \quad .. \quad .. \quad .. \quad .. \quad .. \quad (1)$$

where F is the force in dynes, B the air gap flux-density in gausses, and A is the area in cm². This formula is occurring most frequently in texts, and is apt to be misleading when the assumptions on which it is based are neglected. When saturation in the iron is negligible, equation (1) reduces to

$$F = \frac{B^2 A^2}{8\pi A} = \frac{\phi^2}{8\pi A} = \frac{(0.4\pi NI)^2 A}{L^2} \quad .. \quad (2)$$

where ϕ is the total flux crossing the air gap, NI the ampere turns applied to the circuit, and L the length of the air gap in centimeters.

Equation 2 is a much more accurate form to use when drawing conclusions of the effect on the force of changing physical dimensions. This equation states that if there is no magnetomotive-force drop in the iron, the force varies directly as the face area, directly as the magnetomotive force squared, and inversely as the air gap squared.

It is seldom economical to operate a magnet so low in flux density that the magnetomotive-force drop in the iron can be neglected. In general, then, when saturation is taken into account it is possible to show analytically that there is a pole-face area which will give the maximum pull for any one particular set of conditions. A fast and comparatively accurate method is to solve a circuit by a trial-and-error method, using the saturation curve of the steel involved. The following example illustrates the results obtained by this method : A magnetic circuit was assumed to consist of

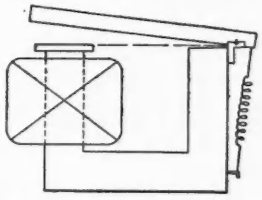

A. Clapper or pivoted armature

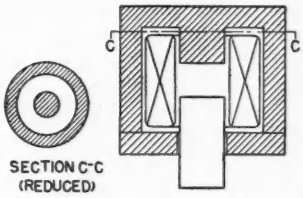

B. Solenoid

Fig. 1

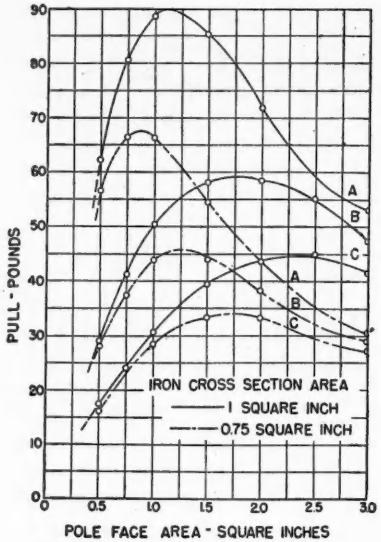

Fig. 2. Effect of pole-face area on pull for various air gaps. A 0.060-inch gap; B 0.090-inch gap; C 0.120-inch gap.

a 10-inch iron path in series with an air gap of 0.080 in., 0.090 in. and 0.120 in. with 2,000 ampere turns applied to the circuit. It was assumed that the ampere turns per in. of iron circuit were constant, and that there was no fringing in the air gap.

In view of data presented later, it will be seen that these two assumptions introduce large errors. They are, however, necessary for a theoretical solution which must be arrived at without the aid of any experimental data. Fig. 2 shows the results obtained. It is of great importance to note that the area for maximum pull varies for different air gaps for it means that each magnet design can be shaped for a particular requirement.

By using the proper core head, the force generated can be kept low in the fully open position and made a maximum at the point where the contact forces begin, so that when the armature once starts to move, it carries the tips through their kiss-and-wipe position without hesitation. Fig. 3 shows the result of varying the length of iron path for the case when the iron cross-section is 1 sq. in., the applied ampere turns 2,000, and the air gap 0.060 in. Fig. 4 shows the effect of impressing various magnetomotive forces on a magnetic circuit of 10-in. iron length, 0.60 in. air gap, and 1 sq. in. cross-section. As the applied magnetomotive force is increased, the pole-face area for maximum pull decreases.

In certain devices such as telephone relays, where the flux density is often very low, the pull of a magnet follows equation 2. The size of the head or pole face can then be increased until the leakage, which is introduced because of the larger head, becomes a limiting factor.

Fig. 5 shows a type of clapper magnet whose proportions are to scale, which was investigated to obtain data on the distribution of flux in the circuit. Search coils consisting of five turns of 0.005E wire were wound on the frame and armature as shown at position a, b, c and d. The coil at b was wound very carefully as close to the air gap as possible, and gave flux values which were taken as the air-gap flux. Data were taken on three such magnets. of the same proportions but of different sizes, which weighed about 8, 12 and 20 ounces. Various ampere turns were applied to the main coil; the flux in each of the search coils was then read for various air gaps, all flux data were taken in an engineering laboratory with a ballistic galvanometer. Using the measured values of density, the magnetomotive-force drop in the iron was found and substracted from the applied magnetomotive force. The net magneto-

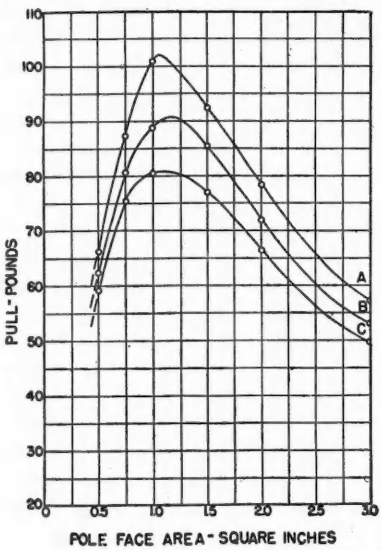

Fig. 3. Effect of pole-face area on pull for various lengths of magnetic paths. A 7.5 inches; B 10.0 inches; C 12.5 inches.

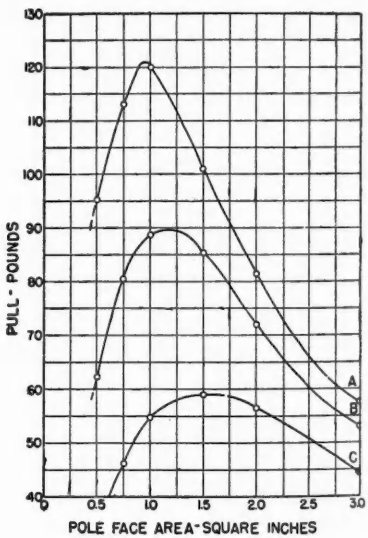

Fig. 4. Effect of pole-face area on pull for various impressed magnetomotive forces. A 2,500 ampere turns; B 2,000 ampere turns; C 1,500 ampere turns.

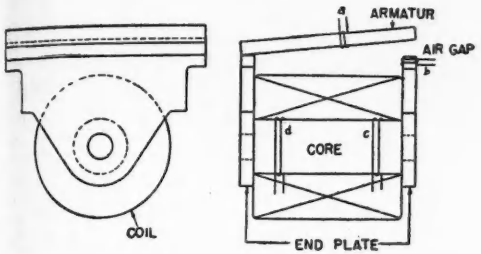

Fig. 5. Form of D.C. magnet used in studying flux variations.

motive force was used to calculate the flux which should cross the air gap, assuming no fringing.

The results obtained are shown in Fig. 6 where A, B and C represent the different sizes of magnet. The equivalent fringing factor which may be taken as the ratio of measured-to-calculated flux is not constant but decreases with increasing density—probably because of local saturation at the edges of the pole face. For magnets A and B the pole-face thickness which, as shown in Fig. 5, is the endplate thickness, was 0.094 in. For magnet C the thickness was 0.125 in. Because of the limited amount of data taken so far on this type of structure, no attempt has been made to determine fringing coefficients as a function of the air-gap dimensions. Fig. 5, however, shows clearly the great error which would result if the air-gap flux is calculated on the basis of no fringing, even for the case where the separation is only 33% of the pole-face thickness.

Table III. shows the ratio of the total measured flux in the core (the average of search coils c and d) to the total measured flux in the air gap. In these three magnets the core was about 25% larger in cross-section than the rest of the magnetic circuit, but the density due to leakage is seen to be very much greater than this increased section can accommodate without excessive magnetomotive-force drop.

These large leakage factors are not peculiar to the type of magnet shown in Fig. 5. Readings obtained on a magnet similar to Fig. 1 A, except with a long thin coil and smaller separation between the legs of the core, showed a ratio of flux measured at the centre of the coil to Flux measured at the pole face of 250% to 333% over the operating gaps of the magnet. In a

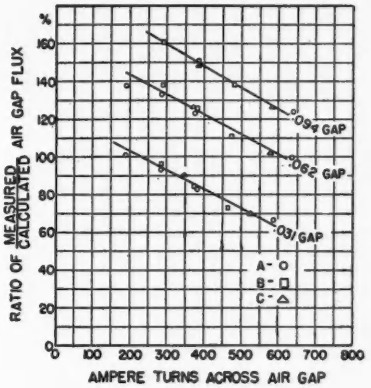

Fig. 6. Ratio of measured to calculated air-gap flux for various impressed magnetomotive forces.

solenoid-type magnet, such as Fig. 1 B, the ratio of maximum flux in the circuit to the useful flux crossing the air gap was found to be 150%.

These leakage figures, of course, vary with the dimensions employed. Leakage flux in D.C. magnetic devices is of an order of magnitude which makes it necessary that their effect be considered in the design.

TABLE III. RATIO OF CORE FLUX TO AIR-GAP FLUX FOR D.C. MAGNETS

Air-Gap Length in Inches	Magnet A	Magnet B	Magnet C
	Impressed Ampere Turns		
	300	400	500
	Core Flux / Air-Gap Flux in Per Cent.		
0.031	190	183	166
0.062	236	224	200
0.094	..	253	225
0.252	..	..	306

ELECTRONIC ELIMINATION OF OIL MISTS

(From *Westinghouse Engineer*, Vol. 3, No. 2, May, 1943, pp. 42-45.)

ONE of the biggest bottlenecks at the outset of the war was the scarcity of machine tools. To increase production the builders of precision grinders have been able to bring the peripheral velocity of grinding wheels up to some 15,000 f.p.m. High-speed thread grinders, and similar equipment of this type, require as much as 18 gallons of oil coolant per minute. The speed and heat of the operation give rise to the oil mist and smoke which has become a serious problem to users of this type of machine tool. At slower speeds, and with but a handful of machines in a large plant, the oil fog problem was not serious, but with literally hundreds of high-speed machines in one enclosure, a veritable cloud of mist is diffused about the plant. Its strength and concentration are such that visibility is lessened, and there is also the possibility that the health and comfort of the operators may be affected. The surfaces of the machines, overhead structures, and floors become slippery from the film of oil which settles on them, and this condition also creates a distinct fire hazard.

The presence of heavy oil mists has a serious deteriorating effect on the factory lighting system, because oil accumulates as a film on the reflectors and lamps. This film also serves as an adhesive to which dirt from the atmosphere clings. Tests show that under these conditions the illumination may drop from 25% to 35% in a short space of time.

The oil also deposits a film on wiring, and because of its adverse effect on the insulation, leads to premature failure. The same holds true for insulation of motors, controls, bus ducts, etc.

Usual Ventilating Systems Ineffective.

Normal ventilating and air-conditioning systems draw air from the building, generally near the ceiling, and re-circulate it along with some fresh air. Seemingly the obvious thing to do was to insert some cleaning or straining device in the central ventilating system. This, however, failed to solve the problem because the oil mist has done its damage before the oil-laden air reaches the ventilating ducts. Individual exhaust ducts running to each machine from the central ventilating

system were considered, but offered many difficulties. In a large plant the maze of ducts would be enormous, and would entail a mammoth ventilating system. Further, it would decrease the flexibility of machine-tool arrangements. The overhead ducts would obstruct the movement of cranes, while the alternative of running the ducts underground is not economically feasible. Possibly the principal risk involved in such an arrangement of overhead ducts is the concentration of a great amount of suspended oil. This would constitute a very real fire hazard which could not be lightly dismissed.

Oil mists and smoke are not removed by the ordinary mechanical filter of the usual ventilating system. The particles, which constitute the mist or smoke vary in size, some being as small as $\frac{1}{10}\mu$ or less in diameter, and cannot be economically removed by mechanical filtering. This precludes the recirculation of the air and represents a great loss in heating energy in winter and cooling in summer. Furthermore, to expel the oil-laden air outside constitutes an economic loss, a fire hazard and a nuisance to the neighbourhood. The failure of the mechanical filters arises, not from their inability to remove the large globules of oil, but from their inability to remove the more finely divided oil particles of 5μ or less. While a large amount of the bulk of the oil in the air is removed mechanically, the mist or oil fog is not materially reduced. Electrostatic removal has proved to be the most economical means of coping with these minute air-borne oil particles.

The Electrostatic Principle.

The principle of electrostatic dust precipitation employed in the Precipitron (Fig. 1) consists of passing the air to be cleaned between high-voltage wires and grounded rods. En route, each foreign particle of dust or oil is given an electric charge. The air containing the charged particles then goes through a system of parallel plates of opposite polarity. The charged particles are drawn to the negative, being helped along by repulsion from the positive plates. In this manner particles, irrespective of size, are removed from the air stream. The cleaned air is discharged practically free of oil and dirt, and is recirculated in the plant. As the particles of oil accumulate on the plates, they form large drops that drip off. The oil thus collected in the drain can be used again as coolant. This recovery of oil represents a real saving.

The Precipitron, using an air velocity of 300 f.p.s., achieves a cleaning efficiency of 90%. The usual measurement of air-cleaning efficiency is made by passing the cleaned air through a white filter paper, the black spot representing unremoved particles. This test could not be applied to oil mist and smoke, as it was found that the paper immediately soaked up the oil and made the test inconclusive. An accurate determination of the efficacy of oil-removal methods was secured by passing the cleaned air through a light beam contained in a chamber having a non-reflecting black lining. A photograph across a beam of light in otherwise dark surroundings (Fig. 2) and in absolutely clean air shows nothing as there is no reflection or refraction from foreign particles. The more particles present in the air, the more the light beam is diffused, and the more distinct the beam of light shows in the photograph. By means of a densitometer (a device for measuring the comparative densities of translucent materials by means of a light beam and photo-electric tube), the comparative strength of the light beam on a photographic negative can be determined, and the efficiency of the cleaning device appraised.

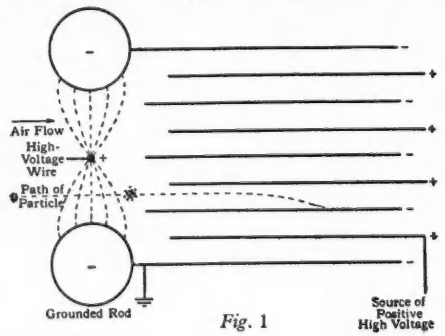

Fig. 1

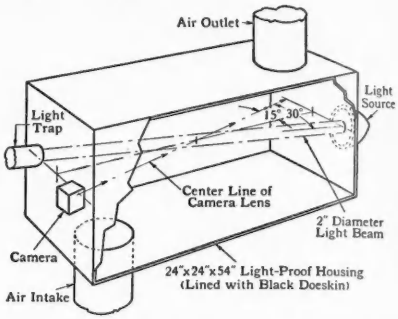

Fig. 2. Tyndall beam test method for determining the efficiency of a ventilating system.

Exhaustive tests were conducted in a gear-grinding plant in Chicago on high-speed precision grinders by Mr. Samuel R. Lewis, Consulting Engineer. An intake was fabricated to suit the needs of the machine and connected to a Precipitron unit. The comparative densitometer readings of the photographs as in Fig. 3 show that the Precipitron was 90% effective while the mechanical filter was less than 14% effective under identical conditions.

Machine-Tool Installation Arrangements.

The preliminary application of the Precipitron to machine-tool installations has taken four general forms. In the first, ducts from intakes on several individual machines enter a larger duct handling this group. Air from the machines is drawn into the common duct by a large unit comprised of a fan and a Precipitron. This, however, necessitated using larger units, the erection of considerable duct work, limitation of machine placement flexibility, and possible interference with material handling.

A variation of this plan used a common fan and exhaust duct for several machines, but each machine was supplied with a separate precipitator, which was energized from a common power plant. With this arrangement the Precipitron unit is smaller, the electronic power tubes supplying the Precipitrons used to best advantage, and the location of machines made more flexible. The flexibility of machine placement was, however, still somewhat hampered, and the overhead duct was bulky.

Another method places the Precipitron in individual cabinets, which also house the fan. Each cabinet is fitted to its own machine. The befogged air is drawn from the machine pick-up into an intake connected to the bottom of the cabinet, through the electrostatic cleaner, and discharged into the room for recirculation. This is a completely mobile arrangement except for the power plant, which is common to several machines.

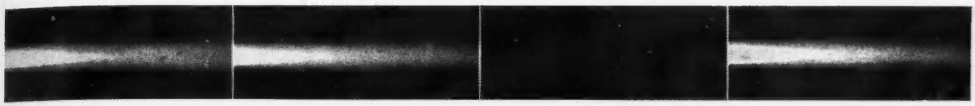

(*a*) Unfiltered exhaust. (*b*) With 4-inch mechanical filters. (*c*) Exhaust passing through a Precipitron unit for individual machine tools. (*d*) Exhaust passing through Precipitron with cells de-energized.

Fig. 3. Photographs of the exhaust from a high-speed grinder taken with equipment shown in *Fig.* 2.

The high voltages are transmitted to each of the Precipitators by separate cables in grounded conduit.

The Individual Unit.

A completely individual unit for each machine tool is the most flexible arrangement. This is a cabinet with self-contained fan and motor, a baffle plate for uniform distribution of the incoming oil-laden air, a mechanical filter to remove the large particles, both solid and liquid, plus the precipitating element. This basic electrostatic unit is rated at about 600 cu. ft. per minute. The integral power plant supplies d.c. ionizing voltage of 13,000 V, and a collecting-plate voltage of 6,000 V d.c. The unit is compact, and stands 50 ins. high and occupies a small floor space of about 20 ins. by 20 ins.

This unit is practically self-cleaning. The oil drains off and carries with it the slight dirt accumulations as they form. The large volume of oil recovered—as much as 5 gallons per machine daily—also passes through and cleans the mechanical filter in a similar manner, making manual cleaning an infrequent operation.

Obviously, the most efficient application of the Precipitron unit to a machine-tool is achieved when the unit is incorporated into the original design of the machine. The present pressing need, however, is to eliminate the great concentrations of oil from plants now in existence. For installation with existing machines, a convenient pick-up is fabricated, and is connected by a duct to the opening at the bottom of the cleaner. Ordinarily the pick-ups are made of sheet-metal, and are designed to provide the maximum intake of mist and the minimum interference with the operation of the machine.

Experience has shown that each application of the unit to existing equipment must be handled as an individual plant problem. In addition to varying plant conditions, there is a wide diversity of types and designs in the highspread thread grinders. To overcome these diversities, a fundamental unit is required that can be adapted to the location and style peculiar to the machine involved merely by designing a proper pick-up. The unit can either be floor-mounted or suspended alongside or above the machine it serves. The coolant oil collected is returned from a pipe connection in the unit to a filtering sump alongside the machine-tool or to a central coolant-filtering location where it is cleaned and piped again to the machines.

Field Experience.

Field experience is still limited, but is sufficient to prove the effectiveness of the Precipitrons. Users in New England, having large numbers of high-speed gear and thread-grinders, have installed this type of air cleaner, both in the unit and central systems. In several instances original installations comprised but a portion of the plant, and the difference between the sections serviced by the Precipitron and those that were not was startling. In one plant all fixtures, walls and machines had been scrubbed down at the time the electrostatic cleaners were installed in a section of the plant. In three weeks the lighting fixtures, overhead structures, etc., over the machines without air cleaners were dripping oil, whereas those over machines equipped with cleaners were clean.

In one plant, in cold weather, the room temperature dropped to 40° F, not for lack of normal heating capacity, but because warm air containing oil mist and smoke had to be discharged from the building, with consequent loss of heat. A Precipitron installation covering these machines resulted in a clean, warm plant because the impurities were eliminated, and the warm air is recirculated with a minimum to make up air and heat expenditure.

SURFACE CURRENTS ON PLASTICS

By R. VIEWEG, VDE, VDI, and H. KLINGELHÖFFER, Darmstadt. (From *Kunststoffe*, Vol. 32, No. 3, March, 1942, pp. 77-81.)

THE specifications of the " Verband Deutscher Elektrotechniker " define " surface current " as the current passing between two knife-edge electrodes (Fig. 1), touching the surface of the material to be tested. This method, which determines the total current passing between the two electrodes, has the advantage of being simple. The proportion of the current passing over the surface (surface current), and through the inside (inside current) is not known. This instrument, therefore, is not suitable for scientific research work.

In order to understand this problem it is necessary to separate the " pure surface current " from the " inner current." There have been frequent attempts to obtain the pure " surface current " by subtracting the pure " inner current " from the total current. The same idea was used in the measurements described below, the current path being shown diagrammatically in Fig. 2.

In the simplest case the current density is uniform throughout the whole insulator. An additional " surface current " is passing over the surface and this can be imagined as the movement of adsorbed ions of a different matter. If the " inner current " density can be measured by means of an auxiliary method, then the difference between the total current passing from electrode to electrode and the " inner current," obtained by means of the auxiliary method, gives the current in the adsorption surface.

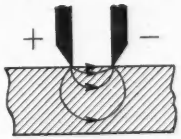

Fig. 1

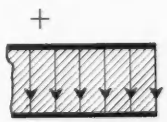

Fig. 2

Actually the conditions become more complicated if the inner layers adsorb the same type of ions as the surface. If, e.g., the increased humidity of the air increases the surface conductivity, then this is accompanied by a simultaneous increase of the inner conductivity. In such a case the increase of surface ions is not entirely due to the surface current, but is only a measure of the surplus of electric conductivity over the value which could be assumed from the inner conductivity. In other words, the surface conductivity is zero if the current passing over the surface is not greater than that passing through any inner layer. We shall see below that this is really a matter of very small currents only.

It should be emphasised that the difference of the currents (amps) is formed for a definite test only. From these values the specific inner resistance (Ω cm.) and the specific inner conductivity (Ω^{-1} cm.$^{-1}$), the specific surface resistance (Ω) and the specific surface conductivity are calculated respectively. This calculation assumes a linear law, namely, that for a plate test specimen of double thickness half of the current is measured.

Circuit and Evaluation of Results.

The current must remain perfectly constant during the measurement of the total current (first measurement) and of the "inner current" (second measurement); the two measurements should be carried out in close succession and repeated as often as possible.

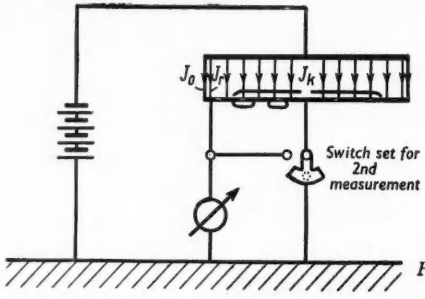

Fig. 3

Fig. 3 shows a circuit diagram which can be recommended, as it fully satisfies all the above requirements. One side of the circular test specimen is covered with a metal (silver) lining. The electrode on the opposite side contains one or several circular gaps. In the first measurement all gaps are bridged, the measuring instrument on the resistance bridge giving the total current $I_k + I_r + I_o$. In the second measurement only the current $I_r + I_o$ in the outside ring is measured, the current I_k of the inside electrode circuit being earthed. I_o is the "surface current," I_r the "inner current" of the ring.

In the graphical evaluation shown in Fig. 4 the currents are plotted against the corresponding surface areas, and thus the currents $I_k+I_r+I_o$ and I_r+I_o are plotted against the total area and the ring surface area respectively. For further measurements several outer rings are connected; thus several points on the curve (Fig. 4) (air humidity $\varphi = 50\%$) are obtained. If only two measurements are carried out, as in the methods used so far, only a straight line can be drawn which approximately represents the total current with varying "inner current." The value of the current obtained from the curve or straight line when the surface area is zero includes no part of the "inner current," but is the required pure "surface current."

The example shown in Fig. 4 shows the extrapolation of the area O for a test piece of type S, at three different

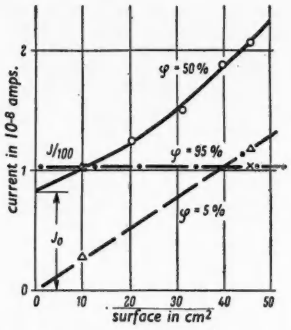

Fig. 4
Graphical determination of surface current Io for plastics. Type S. φ=air humidity.

humidities. At a very low humidity of 5% the straight line passes through the origin, i.e., the surface current is negligible compared with the inner current. On the other hand, with high humidities (e.g., $\varphi = 95\%$) the inner current is negligible, while the surface current is constant for all surface areas. The third curve drawn for a mean humidity ($\varphi = 50\%$) shows the actual purpose of the method. The current through the measuring instrument decreases continuously with decreasing ring surface area; when the surface area reaches the value zero the remaining current is the "surface current" Io.

Results.

The results of several measurements performed on plastics by means of the method described are given below.

Formation of Surface Layers.

Fig. 5 shows a diagram in which the specific surface conductivity is plotted against time. This diagram was obtained by drying a test specimen in a vacuum, then introducing air of high humidity and measuring the increase in surface conductivity. As the time during which the voltage was applied was also important the measurements were taken after the voltage had been applied for two minutes. One minute, as recommended by the VDE specifications, would not have given satisfactory results, the resistance changing considerably just after applying the voltage.

In the examination of the surface conductivity of glass, it was assumed that the carriers of the electricity are adsorbed water ions only. In the plastic type S under discussion, the hydrated ions are of greater importance. Their formation explains the length of time necessary to obtain an equilibrium between the

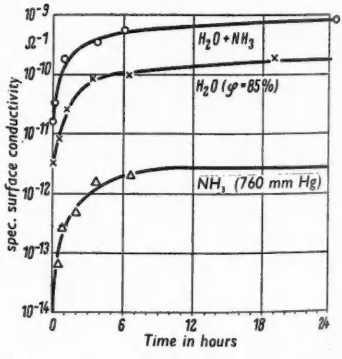

Fig. 5. Formation of a conducting layer.

surface and the surrounding atmosphere, whilst a quicker formation of a conducting layer would have to be assumed if it was a direct effect of the H_2O adsorption, the velocity of which is known from previous adsorption measurements. There is another observation which supports the assumption that the humidity of the air does not directly provide the electricity carriers, but that it only causes the formation of movable particles in the plastic. Thus the surface conductivity in a dry NH_3 atmosphere was found to be very small, whilst it was very high if water vapour was present at the same time. Hence the ions of the adsorbed ammonia seem to be hardly moving themselves, but they aid the transport of the electricity when water is present. This theory, obtained from surface current measurements, is also applicable for the inner conductivity and explains the conductivity as being largely a result of the hydration of aged ions. Besides this, and especially with plastics with softeners, electro-kinetic phenomena have to be assumed.

The Influence of Air Humidity.

The measurement of the surface conductivity at different air humidities throws more light on the problem. It can be seen from Fig. 5 that about 24 hours after a change in humidity a new equilibrium position was obtained. The test specimens, therefore, were exposed each day to a different humidity. The result of the electric measurements at the end of these periods is shown in Fig. 6 for a ground surface, type S, for a plastic standard rod of the same type and for an Igelit specimen.

The absorbed quantities are approximately proportional to the steam pressure, so that with double the steam pressure twice the weight is adsorbed. This rough rule was found for a range of small pressures up to the saturation pressure. If it also applies for the above measurements, then it is noteworthy that a change in steam density of 1 : 1.8 (corresponding to $\varphi_1 : \varphi_2 = 50\% : 90\%$) corresponds to a change in surface conductivity of 1 : 1,000. How is it possible that, after roughly doubling the adsorbed water quantity, the surface resistance is decreased 10^3 times?

Let us assume that the electricity carriers consist of ions which are contained in the plastic and which are made movable by the excess of air humidity. With absolutely dry air there is already an initial conductivity. For the middle curve of Fig. 6 it is estimated to be 10^{-13} to 10^{-12} Ω. The water particles absorbed with increasing air humidity are initially inadequate for all soluble constituents of the plastic; good conducting

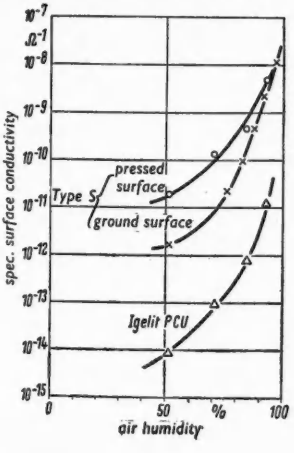

Fig. 6

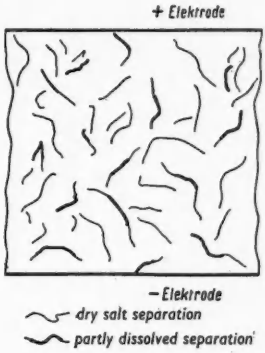

Fig. 7
Sketch of conducting paths. According to H. Stager. Magnification about ×400.

paths will be interrupted by paths of "dry" conductivity. Using Stager's micro-pictures, the conditions can be seen, as shown, diagrammatically, in Fig. 7. If all soluble constituents were in concentrated solution, then a further increase in the water adsorbed could increase the conductivity only by an increased dissociation with a decreasing degree of concentration. The fact that there is such an increase in the dissociation can be seen from the curves in Fig. 6, which gives values 100 and 1,000 times larger than those calculated from a linear increase of the current paths, with a good constant conductivity. On the other hand, according to known measurements, the increase in dissociation is not so considerable that it alone could explain the steep increase of the conductivity, especially with high humidities. One must, however, assume: with increasing air humidity, good conducting paths are formed with solutions very diluted in parts and greatly dissociated; only at high humidities do these conducting paths form closed circuits. If the soluble parts do not form closed chains, then the last step in increasing the conductivity could be achieved by diffusion through the separating parts.

In this respect it is remarkable that, with high humidities, the surface current is so considerable (Fig. 6) that it cannot be neglected, even in the case of long current paths. A comparison of Igelit with plastic type S shows that a considerable improvement can be achieved by using the proper material; with humidities approaching the saturation point, the resistance of different insulating materials tends to be equal. As the last resort electric safety circuits for conducting away the surface currents can be employed.

The test specimens used for the above measurements were cleaned mechanically with great care. Thus the influence of the surface shape was only slight. With type S the conductivities of the plastic were even higher than those of a ground surface. Questions as to the type of surface probably become more important when the surfaces become dirty through use.

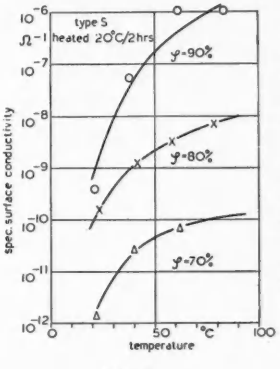

Fig. 8

The Influence of Temperature.

With only a few exceptions the conductivity-temperature curves vary for electron and ion "conductors" respectively. By means of Rasch and Hinrichsen's law, the problem of the ion flow can be understood from the position and steepness of the curves mentioned above. The steepness of the curves obtained by plotting the reciprocal of the temperature T against the logarithm of the conductivity depends on the separating energy E of the ions taking over the charge, the position A of the curve, and on the number and velocity of the electricity carriers. Using this law the conductivity can be expressed by the equation $X = A \cdot e^{-E/T}$

where E depends on the heat of solution of the conductor ions, A depends on the number of ions and the movability which grows with increasing temperature due to decreased friction in the adsorption layer.

As the ions are identical both in the "inner" and "surface" conductivity, E should be the same in both cases; experiments show that this is so for temperatures below 60°, above this temperature, however, the slope of the curve decreases, which is easily explained by the decrease of the adsorption layer at higher temperatures (desorption). The difference in dimension makes a comparison of A for inner and surface conductivity impossible. Correlating, however, an inner layer of 1μ thickness with a surface layer, which can be assumed to be of the same thickness, then for the type S

$$A_1 : A_o = 1 : 10^5,$$

which ought to be due less to the increase of ions than to the considerably smaller surface resistance.

A special increase of ions, as on surfaces dipped into solutions, is not possible, there being no subsequent delivery of ions in the case of water vapour absorption.

ENGINE COOLING PROBLEMS ARISING IN MOTOR CAR DESIGN

By Dr. Ing B. Eckert, VDI/ATG. (From *ATZ Automobiltechnische Zeitschrift*, Vol. 45, No. 10, pp. 270-280. (Part II.)

B. THE FAN.

When considering the power required for liquid cooled engines, often too little attention is paid to the fan. Satisfactory cooling, however, is possible only with a fan of adequate capacity. With the air-cooled engine, the fan is, of course, of paramount importance.

I. The work done in the ducted system.

If we consider the pressure drop of the cooling air on its way from entry into and exit from the bonnet, again for the K-car, we obtain Fig. 9, where the abscissa shows the pressure head $H = \frac{\Delta p}{\gamma}$. Fig. 9 gives the change of the total and static heads along the ducted system. Utilizing the stagnation pressure due to forward speed, the pressure increase is

$$\Delta p_{required} = \rho/2 \left\{ \sum_{i=o}^{i=n} c_{Wki} \left(\frac{\nu_i}{\nu_k}\right)^2 v_k^2 + v_a^2 - v_F^2(1-\zeta) \right\}$$

Herein, $\sum_{i=o}^{i=n} c_{Wki}$ is the sum total of all drag coefficients along the duct, including the cooler.

The thermal change of the cooling air on its way is taken care of by the term $\left(\frac{\nu_i}{\nu_k}\right)^2$, whereby ν_i denotes the the specific volume over part i of the duct. By using Gay-Lussacs' law, one obtains for arbitrary stations i in front of the cooler

$$\left(\frac{\nu_i}{\nu_k}\right)_{front} = \frac{2T_1}{T_1+T_2}$$

and for those behind the cooler

$$\left(\frac{\nu_i}{\nu_k}\right)_{behind} = \frac{2T_2}{T_1+T_2}$$

T_1 = absolute temperature in front of radiator. T_2 = absolute temperature behind radiator. Then, the efficiency of the air duct is

$$\eta_L = \frac{c_{Wko}}{\sum_{i=o}^{i=n} c_{Wki} \left(\frac{\nu_i}{\nu_k}\right)^2}$$

The power required for the fan, when vehicle in motion, is

$$N_G = \frac{V \Delta p_{required}}{\eta_G \cdot 75} = \frac{V}{\eta_G \, 75} \cdot \frac{\rho}{2} \left\{ \sum_{i=o}^{i=n} c_{Wki} \left(\frac{\nu_i}{\nu_k}\right)^2 v_k^2 + v_a^2 - v_F^2(1-\zeta) \right\}$$

$$= \frac{F_k \frac{\rho}{2} v_k^3 \, c_{Wko}}{\eta_G \cdot 75} \left[\frac{1}{\eta_L} - \frac{v_F^2(1-\zeta) - v_a^2}{v_k^2 \, c_{Wko}} \right] \text{H.P.}$$

This equation contains all factors governing the power required for the fan, the member $v_F^2 (1-\zeta)$ takes into account the pressure at the cooling air exit.

To simplify the equation one can neglect the influence of the speed of vehicle, and assume $v_a = 0$. Then, the required power for the fan is

$$N_G = \frac{F_k \frac{\rho}{2} v_k^3 \, c_{Wko}}{75 \cdot \eta_G \cdot \eta_L} = \frac{F_k \frac{\rho}{2} v_k^3 \, c_{Wko}}{75 \, \eta_A}$$

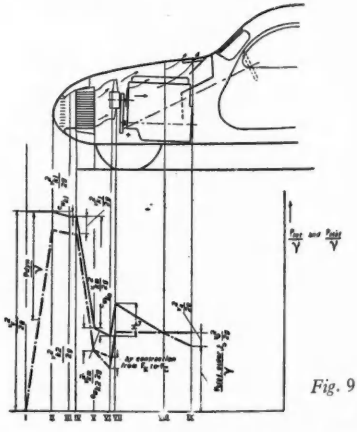

Fig. 9

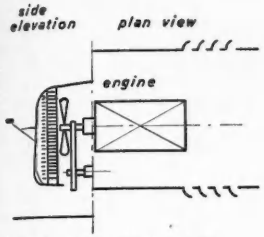

Fig. 10. Present day design.

$$\eta_L = \frac{C_{W_{ko}}}{\Sigma C_{W_{ki}}} = 0.45$$

$\eta_G = 0.50$

$\eta_A = N_L \cdot N_G = 0.225$

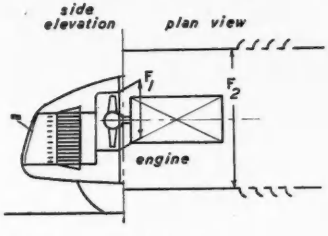

Fig. 11. Lay-out of the K car.

$\eta_L = 0.48$

$\eta_G = 0.80$

$\eta_A = 0.38$

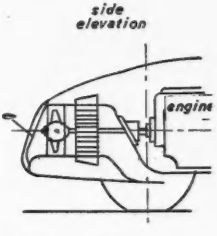

Fig. 12. Ideal lay-out.

$\eta_L = 0.95$

$\eta_G = 0.82$

$\eta_A = 0.78$

Examples given in Figs. 10–12 show how the efficiency of the airducts can be improved. Expressed in figures, the required powers for the respective fans are in the ratio of 1 : 2.05 : 3.45.

The expression for N_G contains ρ, the density of air, which has been taken at sea level and is based on the International Standard Atmosphere (ρ=0.125 kg. sec^2/m^4). However, for desert roads and vehicles in military formation, the change in density due to sand and dust must be taken into account. As a limiting case, at + 60°C, one can assume $\rho = 0.41$ kg. sec^2/m^4. This is a 3.5 times higher figure as compared with the density of pure air. The increase in power required for the fan is of the same order as the increase in density.

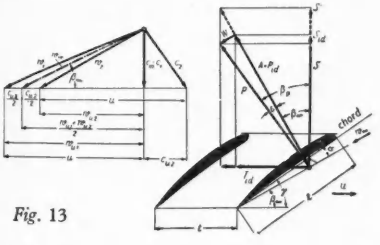

Fig. 13

Velocities :

u, Peripheral velocity ; w, Relative velocity of flow ; c, Absolute velocity of flow.
Index m, Component in meridional direction
Index u, Component in peripheral direction.
Index 1 refers to inlet ; Index 2, refers to outlet ; Index ∞ refers to mean effective conditions.

Forces :

P, Resultant aerodynamic force
A, Lift, component of P perpendicular to w∞
W, Drag, component of P, parallel to w∞
S or Sid, Thrust, component of P or A in axial direction
S", Thrust in inviscid fluid, if peripheral force is T
T or Tid, Peripheral force, component of P or A in peripheral direction
} Index id refers to inviscid fluid.

Linear dimensions :

$t = \frac{D\pi}{z}$ blade spacing — D, outer diameter; l, blade chord length; z, number of blades

Angles :

βp, Angle between P and axis
$\beta\infty$, Angle between w∞ and peripheral direction
α, Angle of incidence

$\epsilon = \beta p - \beta\infty = \frac{C_w}{C_a}$ (glide angle)

$\gamma = \beta\infty + \alpha$, angle between chord and peripheral direction.

II. The Fan.

Fans for cooling air must have a high output as to the volume of air, with a relatively small increase in pressure. For this purpose, preferably, axial flow fans are in use. These belong to the group of the specific high-speed turbo machinery. Their calculation is based on the aerofoil theory.

1. The Calculation of the Fan.

In neglecting radial flow components, the axial flow in the blower can be regarded as if it was taking place on co-axial cylindrical surfaces.

By applying the second Euler turbine equation to the axial flow blower, one obtains the total pressure increase

$$\Delta p_{tot} = \frac{\rho}{2}\left\{ (c_2^2 - c_1^2) + (w_1^2 - w_2^2) \right\} \text{ kg/m}^3$$

(See also Fig. 13).

Hereby the static pressure increase

$$\Delta p_{stat} = \frac{\rho}{2}(w_1^2 - w_2^2) = \frac{\rho}{2}(w_{u1}^2 - w_{u2}^2) \text{ kg.}$$

For the axial thrust of the aerofoil element of db thickness in radial direction, one obtains

$$dS' = db\, t \frac{\rho}{2}(w_{u1}^2 - w_{u2}^2) \text{ kg.}$$

The force in peripheral direction can be calculated by the momentum theorem, thus

$$T = db\, t\, \rho\, c_m (w_{u1} - w_{u2}) \text{ kg.}$$

To obtain the resultant force dR, which is perpendicular to the incident velocity w∞, Kutta-Youkowski's theory for flow through rows of aerofoils is applied

$$dR = dA = \rho\, t\, db\, w_\infty (w_{u1} - w_{u2}) \text{ kg.}$$

According to Eiffel's definition of the lift coefficient

$$C_a = \frac{dA}{\frac{\rho}{2} w_\infty^2\, l\, db}$$

By using the two last equations,

$$C_a\, l = \frac{2 (w_{u1} - w_{u2})\, t}{w_\infty}$$

From Fig. 13

$$w_{u1} - w_{u2} = c_{u2}.$$

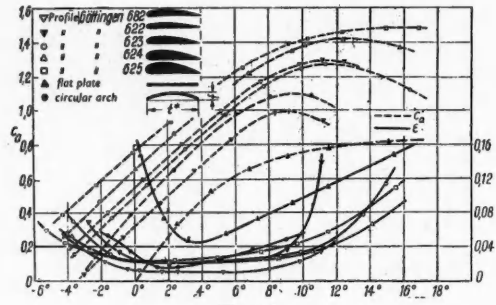

Fig. 14

Again, according to Euler's turbine equation

$$c_{u2} = \frac{\Delta p_{tot}}{\rho u} \text{ m/sec.}$$

Herewith one obtains the equation which is used in dimensioning of axial flow blowers, as

$$c_a \; l = \frac{2 \Delta p_{tot}\, t}{\rho\, u\, w_\infty} \simeq \frac{120 \Delta p_{tot}}{\rho\, n\, w_\infty\, z} = \frac{120\, H_{tot}\, g}{z\, n\, w_\infty} \text{ m.}$$

The equation indicates that for deep or dirty radiators and unfavourable ducting, an increased output is required from the fan. To fulfil this requirement within the limits of economy is not an easy matter, as the fan speed n and the relative speed w_∞ are limited by the permissible noise level, whereas the lift coefficient c_a and the number of blades z are subject to aerodynamical restrictions.

In Fig. 14 a series of aerofoil sections is given as used in fan design. The diagram is taken from Prandtl & Betz, Göttinger Ergebnisse, I.-IV. (1921-1932), and has been corrected for infinite respect ratio.

2. The Fan Efficiency.

The rotor efficiency is defined by the ratio of the thrusts in inviscid fluid to that in viscous fluid. This is

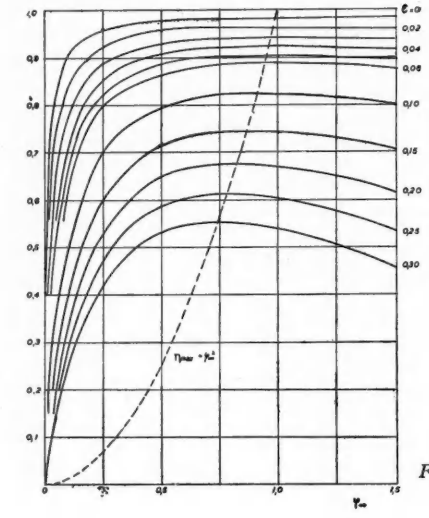

Fig. 15

$$\eta_R = \frac{1 - \epsilon\, \varphi_\infty}{1 + \frac{\epsilon}{\varphi_\infty}}$$

Herein

$$\varphi_\infty = \frac{Cm}{u - c_u/2} = \frac{2\,Cm}{w_{u1} + w_{u2}} \text{ (see Fig. 13),}$$

is a fixed quantity for a given fan. Thus, the efficiency is further dependent on the glide angle E of the blade section chosen. Fig. 15 shows the influence of ϵ on the rotor efficiency. Summing up it is feasible to say that by correct application of theory and test results a fan efficiency of 80% can safely be achieved.

The decrease in fan efficiency due to surface roughness of the blades is negligible within the pressures at which cooling fans operate. Thus die-casting of the blades is a suitable process, requiring no additional machining.

III. The Fan at varying working conditions.

Generally the radiator and the cooling fan are designed for full throttle conditions. This condition corresponds to most strenuous hill-climbing in bottom gear (Fig. 16, point 1). For lesser gradients, e.g., point 2, the speed of the vehicle and the fan speed increase proportionally to the engine speed, i.e., the cooling power is in excess of the amount of heat produced by the engine. The power consumed by the fan increases with the third power of the r.p.m., and at maximum r.p.m. of the engine (point 3) the increase is proportionate to $\left(\frac{n_3}{n_1}\right)^4$. It is the latter condition on which the design of the fan drive is based.

Calculating now, in accordance with Fig. 16, the required pressure increase in the fan, with a view to obtaining a cooling equilibrium at all speeds and fan gear ratios, one obtains Fig. 17. Here again the K-car has been taken as an example.

Should the cooling power required be a minimum value for all speeds, a control of the fan becomes imperative.

IV. Types of Control.

1. Control of Flow of Cooling Liquid.

A control of temperature by throttling the volume of liquid flowing through the radiator or by using switches with a "short circuit" can effect no saving in cooling power. With this type of control, merely, an over-cooling can be avoided.

2. Control of Air Flow.

(*a*) *Throttle control.*—For conditions of delivery by the fan of more air than necessary, shutters can be

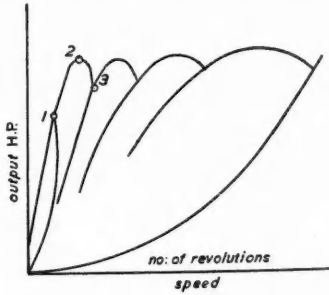

Fig. 16

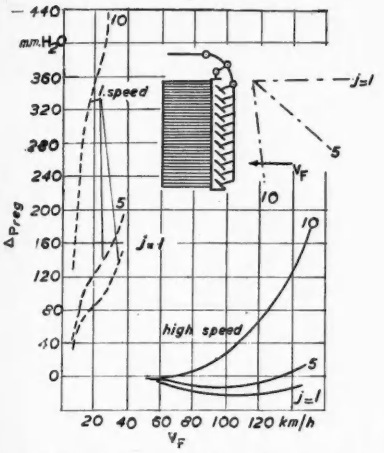

Fig. 17. Required pressure ΔP_{reg}, for various positions of shutter j for two gear conditions, plotted against speed of vehicle V_F, based on the K car.

employed to regain equilibrium. In Fig. 17, for each of the two conditions dealt with there, curves for three shutter positions (j = 1, 5, 10) are shown. In effect, this type of control increases the required pressure of the fan, whereby a balance between available and necessary pressure is obtained. From the point of view of power saving this type of control is unsuitable.

(*b*) *Variable pitch blade control.*—The effect of this type of control is based on the variation of the blade angle of incidence. Corresponding to this change is the change of the blade lift coefficient, and with it the air pressure.

(*c*) *Fan speed control.*—Investigations carried out are in favour of a continuous speed control. It appears therefore that frictional wheel drives transmitting about 10 H.P. would be suitable for fan drives, at least with air-cooled engines; with liquid-cooled engines a somewhat simpler drive would suffice.

This type of control is the only one free from power losses, accordingly there is a minimum value of the power required for the fan.

V. The Open Fan.

With liquid-cooled engines, hitherto mostly open fans have been employed. Owing to the decrease in circulation towards the blade tips, this type of fan is always inferior to the encased type. A good idea about the difference between the two types can be obtained when considering the influence of clearance on a 12-bladed axial-flow rotor shown in Figs. 18 and 19. A chart giving the characteristics of the fan is shown Fig. 20. The influence of variation in blade δ pitch becomes also obvious from the chart. The data refer to a high pressure fan of 300 mm. diameter shown in Fig. 18, 5,400 r.p.m., a rate of flow V = 1.2 m³/sec, and a pressure Δp_{tot} = 225 mm. water column. In Fig. 21 the ratio of the fan pressure at a given clearance s to the maximum pressure at the smallest clearance, is plotted against various values of s. These values, and the corresponding ratios of fan efficiency have been found experimentally. It is clear that the encased fan is by far superior to that without casing. In addition with the former, a better utilization of the cooler frontal area is possible as the pressure gradient over the diagonal of the radiator area is nearly constant.

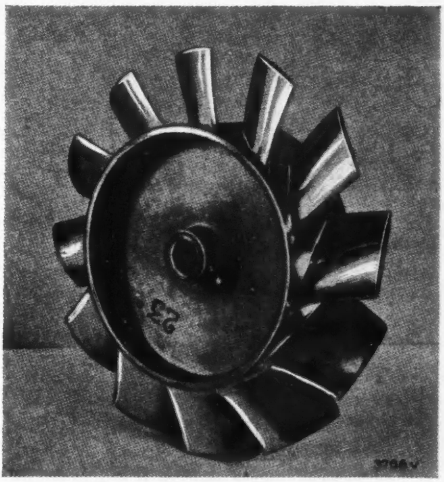

Fig. 18.

VI. The Position of the Fan.

The question whether it is practical to instal the fan in front of the radiator or behind it can be answered in the affirmative for the former position. In this case the fan receives the unheated outer air, and is less loaded. Also the cooling efficiency is increased due to greater turbulence.

(*C*) *The influence of the radiator weight on the power absorbed in cooling.*—The weight of the radiator plus coolant, including the fan and fittings, is about 2 to 3% of the total weight of vehicle. The maximum power necessary for carrying this plant is 1% of the engine power. An increase in weight due to change of depth of cooler has therefore no significance. From the weight point of view the air-cooled auto engine is preferable to the liquid-cooled one. A noticeable influence on the power balance sheet cannot, however, be expected.

(*D*) *Power absorbed in the coolant pump.*—Most of the modern auto-engines use centrifugal pumps, the required power for which is

$$N_p = \frac{V_w \cdot p_w \, \Sigma h}{\eta_p \cdot \eta_m \cdot 75} \text{ H.P.}$$

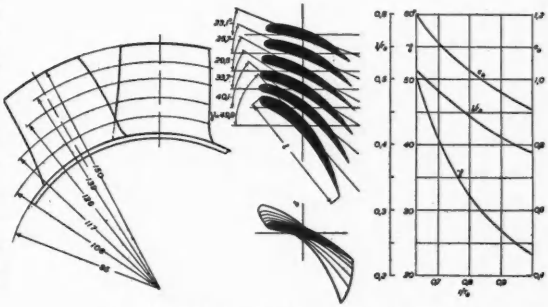

Fig. 19. Blades of fan shown in *Fig.* 18.

$\frac{r}{r_a} = \frac{\text{arbitrary radius}}{\text{outer radius}}$

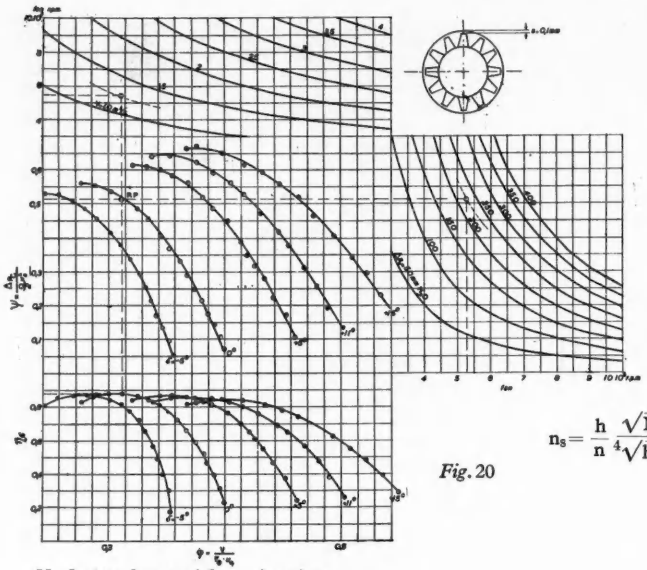

Fig. 20

V_W [m³/sec] rate of flow of coolant,
$\gamma_W = 1{,}000$ [kg/m³] specific weight of water,
($\gamma = 1{,}090$ [kg/m³] for 30% Water + 70% Glycol), percentage referred to volume.
Σh [m] total pumping head.

The required volume of coolant is given by the relation

$$V_W = \frac{Q}{(tw_E - tw_A)\, c_p} \text{ [litre/hour]}$$

($C_p = 1$ [Kcal/Kg °C] for Water,
$C_p = 0.77$ [Kcal/Kg °C] for 30% water + 70% Glycol at 80°C.
percentage referred to volume).

The volume of coolant for a given cooling system should be such as to reach the saturation limit at maximum power. A further increase in volume is undesirable as it is accompanied by an increase in the resistance of the system.

The pumping head Σh is composed of frictional resistances in the engine, Δh_M and, in the tubes of the radiator Δh_K, and of dynamic resistances at entry Δh_E and outlet Δh_A.

$\Delta h_E = \frac{w_E^2}{2g} \lambda_E$ [m] is known as the Borda shock, in which λ is a coefficient of resistance, dependent on the Reynolds' number.

Through contraction at the inlet about 30% of the speed-energy is lost, thus,

$$\Delta h_A = \frac{0.3\, w_A^2}{2g} \lambda_A \text{ [m]}.$$

The total pumping head to be supplied by the pump is then

$$\Sigma h = \Delta h_M + \Delta h_K + \Delta h_E + \Delta h_A \text{ [m]}.$$

This is dependent on the layout of the cooling system, and can only be determined experimentally.

The specific speed for pumps is defined in general by

$$n_s = \frac{h}{n \sqrt[4]{h}} \frac{\sqrt{N}}{} = \frac{n \sqrt{\gamma_w}\, V_w^{\frac{1}{2}}\, h^{\frac{1}{2}}}{h \sqrt{75}\, h^{\frac{1}{2}}} = n \frac{\sqrt{\gamma_w}}{\sqrt{75}} V_w^{\frac{1}{2}}\, h^{-\frac{3}{4}}$$

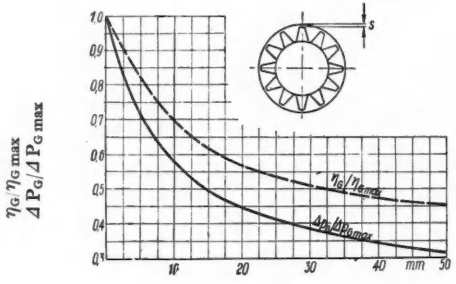

Fig. 21.

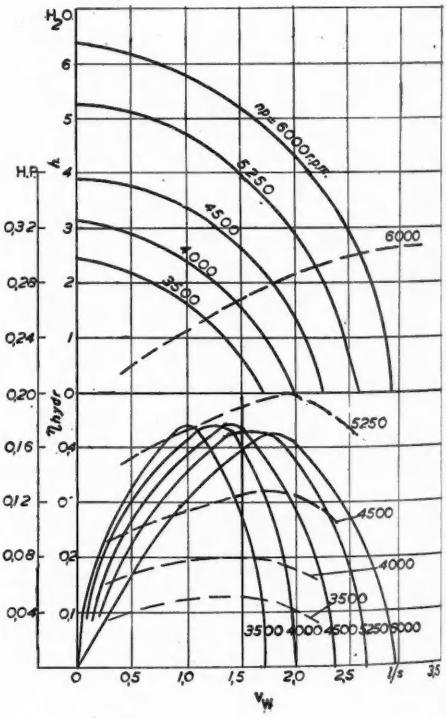

Fig. 22.

If the coolant is water,

$$n_s = 3.65\ n \cdot V_w^{\frac{1}{2}} \cdot h^{-\frac{3}{4}}.$$

Table 1 gives a grading of pumps of normal dimensions (rotor diameter D > 150 mm.) and the attainable efficiencies.

Owing to the smallness of the pumps used in automobiles, the efficiencies are essentially lower.

Fig. 22 shows a characteristic chart for an automobile coolant pump. From this it follows, *inter alia*, that a control of the coolant pump would not result in increased cooling power but rather in pressure losses.

TABLE 1.

Flow	Spec. Speed	Type	Hydr. Efficiency
Radial	50 to 120		0.4 to 0.6
„	120 to 180		0.6 to 0.85
„	180 to 300 (400)		0.7 to 0.86
Axial	> 400 to 1,200		0.75 to 0.88

THE ZEISS-IKON SLOW-MOTION CAMERA

(From " *Flugwehr und Technik*," Vol. 5, No. 1, January, 1943, pp. 24-26.)

SLOW-MOTION cameras were developed during the last war by Messrs. Ernemann, Dresden, for ballistical research work. 35 mm. normal film was used. Messrs. Zeiss-Ikon, after taking over the Ernemann works, continued to develop slow-motion cameras for 35 mm. film, with speeds up to 1,500 pictures per sec., and about two years ago introduced a 16 mm. camera to the market (Fig. 1).

The smaller film made it possible to reach higher speeds, but the 35 mm. size has other advantages, especially for ballistical research.

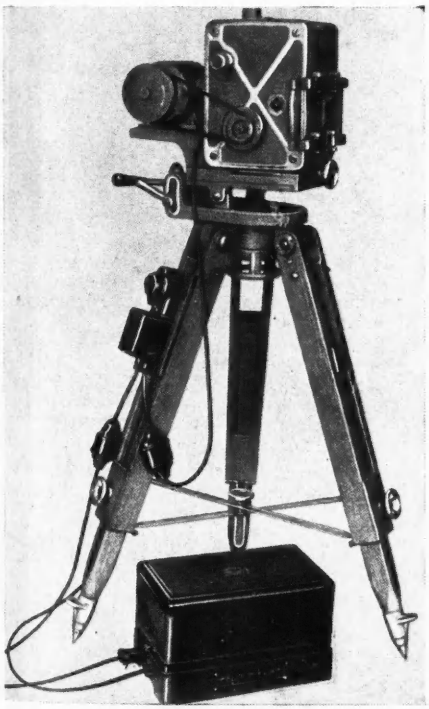

Fig. 1. 16 mm.—film slow-motion camera with electric drive and time recording device.

While normal cameras use an intermittent film movement, this is not possible with the fast movement of the film in slow-motion cameras. The film movement on such cameras is continuous, and an optical compensating device is used to move the image in synchronism with the film. The Zeiss-Ikon camera uses a ring of mirrors for this purpose, which rotates at such a speed as to keep the velocity of the picture equal to the velocity of the film.

The light passes through an aperature at the front of the camera, and is reflected upwards by the mirrors (Fig. 2). An objective with fixed focal length is placed between the mirrors and the film. The camera object

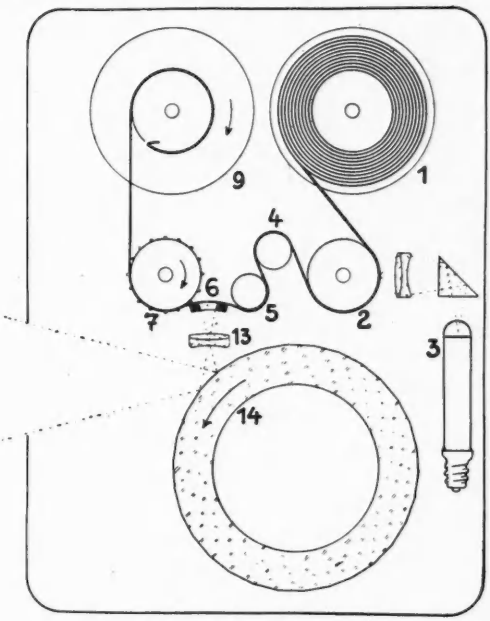

Fig. 2. Diagrammatic view of the slow-motion camera.

1 Supply spool
2 Guide roller
3 Time recording device (Spot neon lamp)
4, 5 Guide rollers
6 Picture gate
7 Sprocket wheel
9 Take-up magazine
13 Objective
14 Mirror ring

distance is adjusted by special auxiliary lenses placed before the mirror ring, giving distances from 0.20 m. to ∞. A slot diaphragm on the objective ensures maximum reduction of picture movement. The objective used is a Zeiss-Sonnar 1 : 2, f 1.8 cm. To make long shots with an increase in magnification, a telephoto system is provided increasing the focus from 1.8 to 7.5 cm. The same objective may be used with additional tubular extensions to take pictures at magnifications of 1 : 1, 1 : 2, or 2 : 1. This arrangement is particularly useful for filming watch movements and similar small details.

There are three methods of driving the camera :

(1) By handcranking for speeds up to 100 pictures per second ;
(2) By spring motor, for speeds of 250, 500 and 1,000 pictures per second ; and
(3) By electric motor, for speeds of 500, 1,000, 1,500 and 3,000 pictures per second, when using full size 18 × 24 mm. frames.

A recent development provides a 60-mirror ring which may be used instead of the normal 30-mirror ring, and the individual pictures have only half normal height. With spring motor, maximum speed thus becomes 2,000 pictures per second, and with electric drive, 6,000 pictures per second. Projectors for these half-size frames are available.

The camera is equipped with an optical viewfinder with parallel correction. A special focussing magnifier is available for focussing directly on the film, which is especially useful for filming at short distances with the objective attachment.

When using the electrical drive, the camera is mounted on a special strong stand with a turnable and inclined head. For fine focussing there is a micrometer adjustment which moves the camera along its optical axis by 100 mm. This is an advantage for close-up work.

The camera is equipped with a time-recording device, based on a tuning fork. Time marks may be recorded every 1/1,000 and every 1/50 sec.

Special slow-motion camera film made by Zeiss-Ikon is used in length of 20 or 25 m. It must be coated with a thin wax layer on the edges ; this is done in a special waxing and re-reeling apparatus.

BACK AXLE DRIVE OR ALL WHEEL DRIVE FOR HEAVY LORRY WITH TRAILER

By P. STROHHACKER VDI, Backnang. (From *ATZ*, Vol. 45, No. 13, July, 1942, pp. 360-366.)

WHEN taking into account the forces acting on a lorry, the equilibrium condition of the various parts must be borne in mind, but special consideration must be given to the line of action and point of application of the forces.

External forces, such as the traction force at the trailer coupling, the rolling resistance, inertia and braking forces, and wind resistance, influence to a smaller or greater extent the axle pressures (according to the distance between the line of action and the road, the load on one axle is shifted on to the other axle).

The rolling resistance, therefore, has no influence on the axle pressures, as it acts at the point of contact of tyres with the road.

With heavy lorries with trailer the traction force is of greatest importance, all the other external forces being negligible.

The influence of the traction force on the load acting on the driving axle is examined below. With multiple axle drives it is desirable that the work done by the driving axles equals, at least within the separate axle groups, the ratio of the static loads on the axles.

From Fig. 1, the torque exerted by the back axle is $M_b = Z.i$.

Depending on the distance between the two axles e, the decrease of load E on the front axle and the additional load on the back axle due to the above moment is

$$E = B = \frac{Z.i}{e}$$

Four-wheel Lorry with Back Wheel Drive.

With heavy lorries with trailer it is important that the tractive force is approximately equal to the weight of the lorry. The coefficient of friction μ between the tyres and a dry concrete road (Reichsautobahn) and a rough asphalt road, is 0.90 and 0.80 respectively.

In considering the four wheel lorry with back wheel drive (Fig. 1), the following static axle loads are assumed :—

Load on front axle	..	2,500 kg.
Load on back axle	..	7,500 kg.

The maximum tractive force at the towing hook is calculated from the formula where—

$$Z = \frac{e\,(G_H\,.\,\mu - G\,.\,f)}{e - i.\,\mu}$$

where

Z = tractive force at the trailer coupling in kg.
G = total weight of lorry in kg.
G_H = load on driving axle in kg.
e = distance between wheels in m.
f = rolling resistance.
i = distance between towing hook and road in m.
μ = coefficient of friction (road—tyre).

The load on the back axle is considerably increased by the tractive force Z. Hence also the maximum tractive force increases ; with the values shown in Fig. 1 and $\mu = 0.9$, we get Z = 8,300 kg.

The dynamic axle loads, i.e., the loads when the tractive force is acting, are :

Dynamic load on front axle	600 kg.
Dynamic load on back axle	9,400 kg.

The total weight, naturally, remains throughout,

G = 10,000 kg.

As long as the lorry is used for traction, the load on the front axle of 600 kg. is, for such limiting cases,

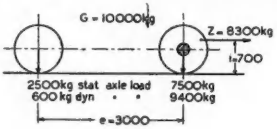

Fig. 1

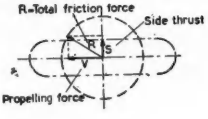

Fig. 2

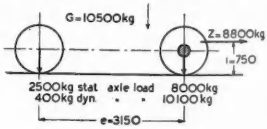

Fig. 3

perfectly sufficient, the loss in propelling force, in the case of a side thrust, being only very small.

According to W. Kamm, the friction force acting on the driven wheel is distributed as shown in Fig. 2. Recent examinations, carried out by Prof. W. Kamm at the Technische Hochschule Stuttgart, show that the above rule is only true for wheels that are stiff in their vertical plane. This, however, should not make a great deal of difference in the considerations below, as the friction force is chiefly used as propelling force.

In the example shown with a side thrust of 2,000 kg., the propelling force of 8,000 kg. would be reduced by 300 kg. only.

The considerable load of dislocation from the front axle to the back axle (Fig. 1) shows that an additional front wheel drive would not be satisfactory as with the same total weight and a coefficient of friction $\mu = 0.9$ (Fig. 1) a maximum tractive force

$$Z = (G_H . \mu - G.f)$$
$$Z = 10{,}000 \times 0.9 - 10{,}000 \times 0.02$$
$$Z = 8{,}800 \text{ kg.}$$

is obtained.

This traction force can also be obtained by increasing the weight of the lorry by 500 kg. (In order to fulfill the requirements § 35 of the StVZO, the distance between the axles must be increased to 3,150 mm.).

With the usual type of lorry the load on the front axle is about 3,000 kg. Assuming a tractive force of 8,000 kg., and the height of the towing hook above the road to be 600 mm., then the decrease of load on the front axle is

$$E = \frac{8{,}000 \times 0.6}{3} = 1{,}600 \text{ kg.}$$

The dynamic load on the front axle is

$$P_{dyn} = 3{,}000 - 1{,}600 = 1{,}400 \text{ kg.}$$

For such a small axle load a front wheel drive would not be justified.

For country vehicles, of course, a front wheel drive is essential, because the non-driven front wheels, when going around in curve, lock the vehicle, thus a great part of the propelling force being lost. Furthermore, with such vehicles used in the country, no large dislocations of the load from one axle to the other take place, these vehicles with wheel drive usually not being used in conjunction with trailers.

Six-wheel Vehicles with Four-wheel Drive.

The arrangement shown in Fig. 4 is used for vehicles of reasonable length designed for not too large tractive forces, with non-driven front axles which are cheap to manufacture, and which have axle loads according to the standard specifications (StVZO). The back axle drive must, however, be so designed that under no condition can a dislocation of the loads on the two back axles take place. Because of this, an examination of various four-wheel drive designs is justified, the uniform distribution of the tractive force on the driven axles being of special interest.

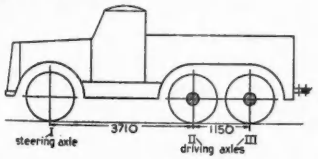

Fig. 4

Fig. 5, shows that the forces acting at the circumferences of the tyres are taken up by the ball heads A and B of the propeller tubes. The ball head A rests against the frame of the vehicle, thus through the point A the tractive force $Z = Z_2 + Z_3$ acts on the two axles.

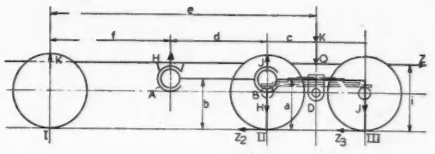

Fig. 5

The frame of the vehicle rests on the front axle I, and is also supported at the pivot D of the leaf springs which rest on the axles II and III, thus giving equal back axle loads.

Assuming that there is a differential built in between the driven axles II and III resulting in a torque ratio 1/1, the following equations are obtained:

$$Z = Z_2 + Z_3 \quad .. \quad (1) \qquad K = \frac{Z\,(i-b)}{e} \quad .. \quad (2)$$

$$H = \frac{Z_2 \,.\, b}{d} \qquad J = \frac{Z_3 \,.\, a}{c}$$

hence following equations are obtained:

$$\frac{Z_2}{\mu} = \frac{Q}{2} + H - J - \frac{H.f}{2e} + \frac{K}{2} \quad .. \quad .. \quad .. \quad (3)$$

$$\frac{Z_3}{\mu} = \frac{Q}{2} + J - \frac{H.f}{2e} + \frac{K}{2} \quad .. \quad .. \quad .. \quad (4)$$

As $Z_2 = Z_3$ and $Z = 2Z_2$ we get from equation (3)

$$Z_2 = \frac{Q}{2\left[\frac{1}{\mu} - \frac{b}{d} + \frac{a}{c} + \frac{b.f}{2e.d} - \frac{(i-b)}{e}\right]} \quad .. \quad (5)$$

As $Z = 2Z_2$

$$Z = \frac{Q}{\frac{1}{\mu} - \frac{b}{d} + \frac{a}{c} + \frac{b.f}{2e.d} - \frac{(i-b)}{e}} \quad .. \quad (6)$$

As in the usual construction $a = b$ and $d = c$

$$Z = \frac{Q}{\frac{1}{\mu} + \frac{a.f}{2e.d} - \frac{(i-a)}{e}}$$

The decrease of load on the front axle

$$E_1 = K + \frac{H\,(e-f)}{e}$$

$$E_1 = \frac{Z\,(i-b)}{e} = \frac{Z_2 .\, b\,(e-f)}{d\,e}$$

As $Z_2 = \frac{Z}{2}$

$$E_1 = \frac{Z\,[2d\,(i-b) + b\,(e-f]}{2ed} \quad .. \quad .. \quad (7)$$

If the main differential is locked or if it is not present, the driving forces Z_2 and Z_3 are distributed according to the dynamic loads on the axles.

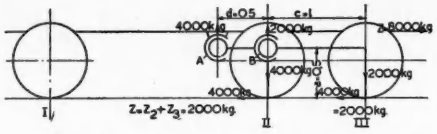

Fig. 6. Axle drive with ball head arrangement, different lever arms d = 0.5c, resulting in equal dynamic axle loads.

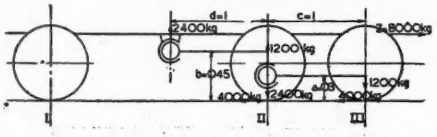

Fig. 7. Axle drive as in Fig. 5, but a = 0.3 and b = 0.45 give equal dynamic axle loads.

The following example is to illustrate the limiting case where there is no load on axle II, and the total torque is exerted by axle III. The assumptions are :

Q = 11,000 kg.
Static load on axle II = 5,500 kg.
Static load on axle III = 5,500 kg.

The load on axle III increases with increasing Z_3, and the engine torque is distributed according to the instantaneous dynamic axle loads. If, therefore, $Z_3 = 9.200$ kg., $\frac{a}{c} = 0.6$, and i = a = b, the decrease in load on axle II—

$$E_{II} = 9{,}200 \times 0.6 = 5{,}500 \text{ kg.}$$

This corresponds to a static axle load, the dynamic axle being zero. Thus no torque is being extered by axle II.

By clever arrangement of the lengths c and d additional loads acting on both axles each being 2,000 kg., are obtained (Fig. 6). The decrease of load at the ball head B due to axle III is $4{,}000 \times 0.5 : 1 = 2{,}000$ kg., and the force on axle III is 2,000 kg. By decreasing the distance d a supporting force $4{,}000 \times 0.5 : 0.5 = 4{,}000$ kg. is obtained. The actual force, therefore, at the ball head B is 4,000—2,000 = 2,000 kg. which is equal to the load on axle III.

The same effect can be obtained with different distances a and b (Fig. 7). If both methods shown in Figs. 6 and 7 are combined suitable conditions for design can be obtained.

The tractive force Z for a ball head arrangement shown in Fig. 8 is obtained in the following way :

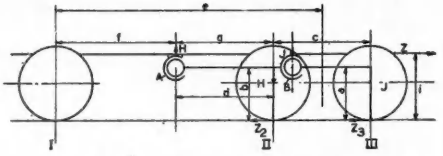

Fig. 8. Ball head arrangement where ball B is not at the centre line of axle II.

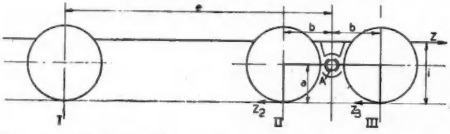

Fig. 9. Both axles are supported at point A. Circumferential force Z_2 decreases load on axle II, Z_3 increases load on axle III.

Assuming $Z_2 = Z_3$ (differential), a = b, $Z = Z_2 + Z_3$, $Z = 2Z_2 = 2Z_3$

$$\frac{Z_2}{\mu} = \frac{Q}{2} + \frac{Z_2 a}{d} - \frac{Z_3 a g}{c d} - \frac{Z_2 a f}{d e 2} + \frac{Z_3 a g f}{c d 2e} - \frac{Z_3 a f}{c 2e} + \frac{Z (i-a)}{2e}$$

$$Z_2 = \frac{Q}{2\left[\frac{1}{\mu} - \frac{a}{d}\left(1 - \frac{g}{c} - \frac{f}{2e}\right) - \frac{a}{e}\left(\frac{f g}{2 c d} - 1 - \frac{f}{2c}\right) - \frac{i}{e}\right]} \quad (8)$$

and as $Z = 2Z_2$

$$Z = \frac{Q}{\frac{1}{\mu} - \frac{a}{d}\left(1 - \frac{g}{c} - \frac{f}{2e}\right) - \frac{a}{e}\left(\frac{f g}{2 c d} - 1 - \frac{f}{2c}\right) - \frac{i}{e}} \quad (9)$$

If the distance between axle II and ball head B (Fig. 8) is greater than 50 mm., then no improvement is achieved by using different lever arms, as shown in Figs. 6 and 7.

With a construction shown in Fig. 9 assuming a torque distribution by means of a main differential

$$\frac{Z_2}{\mu} = \frac{Q}{2} - \frac{Z_2 a}{b} + \frac{Z (i-a)}{2e}$$

but $Z = 2Z_2 = 2Z_1$

therefore $$Z_1 = Z_2 = \frac{Q}{2\left[\frac{1}{\mu} + \frac{a}{b} - \frac{(i-a)}{e}\right]} \quad .. \quad (10)$$

and $$Z = \frac{Q}{\frac{1}{\mu} + \frac{a}{b} - \frac{i-a}{e}} \quad .. \quad .. \quad (11)$$

Without equalization of the torques of the two driving axles

$$Z_2 = \frac{Q \mu (b - \mu a)}{2 b} \quad .. \quad .. \quad (12)$$

$$Z_3 = \frac{Q \mu (b + \mu a)}{2 b} \quad .. \quad .. \quad (13)$$

where, however, the influence of the traction force 2 is not accounted for.

Putting Q = 11 tons,
μ = 0.9 ,,
a = 500 ,,
b = 575 ,,

then $$Z_2 = \frac{11 \times 0.9\,(575 - 0.9 \times 500)}{2\,575} = 1.07 \text{ tons}$$

$$Z_3 = \frac{11 \times 0.9\,(575 - 0.9 \times 500)}{2.575} = 8.83 \text{ tons.}$$

Thus, in such a construction the axle loads are very unevenly distributed ; the axle drive has to be designed for the largest force Z_3, unless a differential for both axles is provided, in which case, however, a small maximum tractive force is obtained (equation 11).

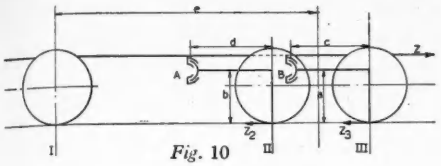

Fig. 10

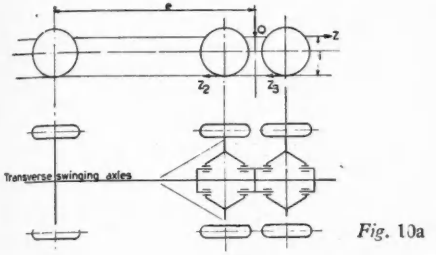

Fig. 10a

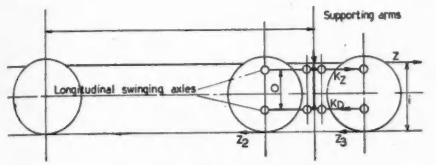

Fig. 10b

Fig. 10 shows a construction where both ball heads A and B are directly suspended from the frame of the vehicle. If the lever arms a, b and e, d respectively are made equal, then the additional axle loads are equal. This, of course, is only the case if both driving axles are loaded by a leaf spring, which in turn is loaded in the middle between the two axles by the frame.

If the driving axles are transversally or longitudinally swinging axles (Figs. 10a and 10b), the tractive force Z can be calculated from the following formula :

$$Z = \frac{Q}{\frac{1}{\mu} - \frac{i}{e}} \quad \text{or} \quad Z = \frac{Q\,\mu\,e}{e - i\,\mu}$$

This is the same equation as that for the four-wheel lorry. The decrease of load on the front axle and the increase of load on the back axle is calculated by

$$E = \frac{Z\,i}{e}$$

No bending moments are being exerted on the frame as in the case of the ball head arrangement, for the circumferential forces at the tyres are only exerting a torque which is being balanced by compressive and tensile forces in the supporting arms (Fig. 10b) acting on the frame.

The forces in the supporting arms are found from the following equations :

$$K_D = K_Z = \frac{Z_2\,i}{o} \quad \text{or} \quad \frac{Z_3\,i}{o}$$

The preventing of load dislocation from one back axle to the other is also of great importance for the braking of a lorry. The types of design, that give equal axle loads during driving, also give equal axle loads during braking. The load on the two back axles is decreased according to the increase of load on the front axle. Table I. gives the maximum tractive forces (on a plane road) and their influence on the loads acting on the front and back axle springs for the constructions discussed. The rolling resistance, being only a small percentage of the maximum tractive force, is neglected.

Comparing the six-wheel lorry with four-wheel drive in Fig. 11, and the four-wheel lorry with four-wheel drive shown in Fig. 12, the following picture is arrived at :

In Fig. 11 the static front axle load is 3,200 kg., and each static back axle load is 5,500 kg. With a coefficient of friction $\mu = 1$, the following dynamic axle loads are obtained :

Table I. Examined four wheel drives Equations giving maximum tractive forces, decrease of load on back axle, and decrease or increase of load on back axle spring due to tractive force

Axle Type I non driven steering axle II and III driven axles	Maximum Tractive force Z Differential between the two driven axles	For shown example const x	Decrease of load on front axle	For shown example const y	%	Decrease or increase of load on back axle spring	For shown example const q	%	Notes
	$Z=\frac{Q}{\frac{1}{\mu}+x}$ $x=\frac{a}{2ed}\cdot\frac{i-a}{e}$	+0133	$E_1=Z\cdot y$ $y=\frac{2d(c-b)+b(e-f)}{2\cdot d\cdot e}$	0129	129	$E_H=Z\cdot q$ $q=\frac{af}{2de}\cdot\frac{i-a}{e}$	-0115	115	
	$Z=\frac{Q}{\frac{1}{\mu}+x}$ $x=\frac{a}{d}\left(\frac{a}{c}-1+\frac{f}{2e}\right)+\frac{a}{2e}\left(\frac{f\cdot a}{2cd}-1+\frac{f}{2c}\right)\frac{i}{e}$	+0144	$E_1=Z\cdot y$ $y=\frac{(c-b)}{e}\frac{b(e-f)}{2de}+\frac{b(c-d)e-f}{2\cdot c\cdot d}$	0140	140	$E_H=Z\cdot q$ $q=\frac{af}{2de}\cdot\frac{i-a}{e}$	-0167	167	With locked or non existing differential $Z_3 > Z_2$ Z_3 can = Z and Z_2=0, even if μ is equal for both driving axles.
	$Z=\frac{Q}{\frac{1}{\mu}+x}$ $x=\frac{a}{b}-\frac{i-a}{e}$	+0182	$E_1=Z\cdot y$ $y=\frac{i-a}{e}$	0047	47	$B_H=Z\cdot q$ $q=\frac{i-a}{e}$	-0047	47	
	$Z=\frac{Q}{\frac{1}{\mu}+x}$ $x=\frac{a}{c}-\frac{b}{d}+\frac{b\cdot f}{2ed}-\frac{(i-b)}{e}$	-0115	$E_1=Z\cdot y$ $y=\frac{2d(c-b)+b(e-f)}{2de}$	0163	163	$E_H=Z\cdot q$ $q=\frac{af}{2de}\cdot\frac{(i-a)}{e}$	-0142	142	If μ is equal for both driving axles, the tractive force is distributed on both axles, even with locked or non existing differential, the dyn axle loads being equal. If μ=0 at one axle, the engine torque is fully (according to μ) transmitted through the other axle
	$Z=\frac{Q}{\frac{1}{\mu}+x}$ $x=\frac{a}{c}-\frac{2b-a}{d}\cdot\frac{f(2b-a)}{2de}(e-f)$	-0115	$E_1=Z\cdot y$ $y=\frac{i-b}{e}\frac{b(e-f)}{de}\frac{a(e-f)}{2de}$	0164	164	$E_H=Z\cdot q$ $q=\frac{f}{2d}\left(b-\frac{a}{2}\right)\frac{i-a}{e}$	-0150	150	
	$Z=\frac{Q}{\frac{1}{\mu}+x}$ $x=\frac{b}{d}\left(\frac{af}{2e}\right)$	-0154	$E_1=Z\cdot y$ $y=\frac{b}{2de}(e-f)(e-1)\cdot\frac{i-b}{e}$	0163	163	$E_H=Z\cdot q$ $q=\frac{af}{2de}(e-f)\cdot\frac{i-a}{e}$	-0180	180	
	$Z=\frac{Q}{\frac{1}{\mu}+x}$ $x=\frac{i}{e}$	-0164	$E_1=Z\cdot y$ $y=\frac{i}{e}$	0164	164	$B_H=Z\cdot q$ $q=\frac{i}{e}$	-0164	164	Equal dyn axle loads
	$Z=\frac{Q}{\frac{1}{\mu}+x}$ $x=\frac{i}{e}$	-0164	$E_1=Z\cdot y$ $y=\frac{i}{e}$	0164	164	$B_H=Z\cdot q$ $q=\frac{i}{e}$	-0164	164	A driven axle can be overloaded only by 8·2% of Z (μ=0·9).

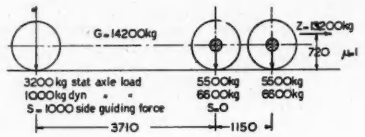

Fig. 11

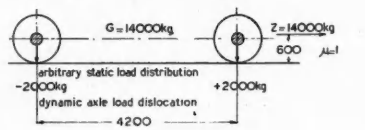

Fig. 12

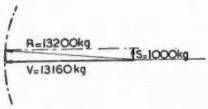

Fig. 13

Front axle .. 1,000 kg. Both Back axles .. 13,200 kg.
The maximum tractive force Z = 13,200 kg.

For the sake of simplicity the rolling resistance was neglected, only a comparison of the traction force being required. For the front axle a side thrust S of 1,000 kg. is obtained. The propelling force decreases (Fig. 13) with a side thrust of 1,000 kg., although the driving axle has to take up such a thrust.

Fig. 12, the lorry with all wheel drive has, under the same conditions as those in Fig. 11, a tractive force of 1,400 kg., *i.e.* only 800 kg. larger than that if the lorry in Fig. 11. It should be noted that when fully using the friction force for the propelling force there is no side thrust. Fig. 14 gives the same construction as that in Fig. 11, the only difference being that the distance between the two back axles is increased to 1,400 mm. Then, according to specifications (§ 35 StVZO) back axles loads of 6,000 kg. each, i.e., a total of 12,000 kg., are permissible. The lorry weight is 14,500 kg., this being only 500 kg. more than the weight of the lorry with all wheel drive (Fig. 12).

With equal static axle loads (Fig. 15), a tractive force of 14,000 kg., and a towing hook 600 mm. above the road, axle load dislocations of ± 2,000 kg. are obtained; thus, the dynamic loads on the front and the back axles are 7,000 — 2,000 = 5,000 kg. and 7,000 + 2,000 = 9,000 kg. respectively. Corresponding to these dynamic axle loads the engine torque is distributed in the ratio 9 : 5.

Another possibility is to have initially different static axle loads (as shown in Fig. 16), so that with the maximum tractive force equal dynamic axle loads are obtained. The disadvantage of this arrangement is that for no load condition the steering axle is subjected to a comparatively high load.

A further possibility of distributing the static axle loads is shown in Fig. 17. According to the specifications (StVZO) axle loads of 9,000 kg. are permissible with lorries of 14,000 kg. total weight. This arrangement would have the advantage that the front axle could be equipped with single tyres only. With a 14,000 kg. tractive force the dynamic axle loads are:

Front axle .. 3,000 kg.
Back axle .. 11,000 kg.

Strictly speaking, for each tractive force Z applied at the towing hook of the lorry with an all-wheel drive, the torque would have to be distributed according to the dynamic axle loads by means of the differential. Such differentials are, so far, not known, and are probably not simple in design. In practice it is found sufficient if the engine torque is distributed according to the maximum tractive force by the differential. Nevertheless, it is shown by the following calculation that the total weight of 14,000 kg. is not fully utilized (u = 0.5), if the torque distribution takes place according to the maximum tractive force (Fig. 15). The tractive force should be $Z = 1400 \times 0.5 = 7{,}000$ kg. The correct tractive force is obtained, however, from the following equation, Z_2 being the circumferential force at the tyre of the back axle:

$$Z_2 = \frac{G_2}{\frac{1}{\mu} - \frac{i}{e} - \frac{i}{e\,\ddot{u}}}$$

where G_2 = static back axle load in kg.,
e = distance between axles in m,
i = distance of towing hook above road,
μ = friction coefficient,
$\ddot{u}$ = ratio of torque distribution in differential,
Z_1 = circumferential force at tyre of front axle in kg.

$$Z_1 = \frac{Z_2}{\ddot{u}}$$

Taking the values given in Fig. 15

$$Z_2 = \frac{7{,}000}{\frac{1}{0.5} - \frac{0.6}{4.2} - \frac{0.6}{4.2 \times 1.8}} = 3{,}950 \text{ kg.}$$

$$Z_1 = \frac{3{,}950}{1.8} = 2{,}200 \text{ kg.}$$

Total tractive force Z = 6.150 kg.
The coefficient of friction at the

Front axle .. $\mu \dfrac{2{,}200}{7{,}000 + 880} = 0.36$

Back axle .. $\mu \dfrac{3{,}950}{7{,}000 + 880} = 0.5.$

In contrast to this, for the six-wheel lorry with four-wheel drive (Fig. 14), taking $\mu = 0.5$, the maximum tractive force is obtained by means of the following equation:

$$Z = \frac{G_2}{\frac{1}{\mu} - \frac{i}{e}} \qquad Z = \frac{12{,}000}{\frac{1}{0.5} - \frac{0.62}{4.35}}$$

$$Z = \sim 6.500 \text{ kg.}$$

In this case the all-wheel driven lorry has a 5½% smaller tractive force.

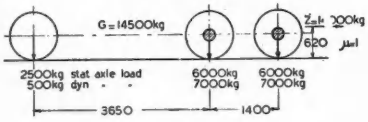

Fig. 14

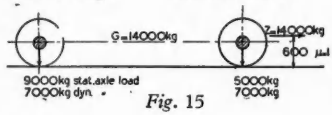

Fig. 15

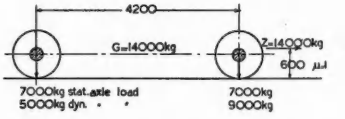

Fig. 16

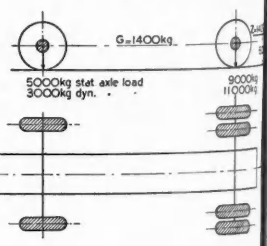

Fig. 17

TECHNICAL NEWS

Announcements in this section include News relating to British Firms, and on Equipment produced by British Manufacturers.

Available literature may be secured by addressing a request to the advertising department of "The Engineers' Digest," or by writing direct to the manufacturer and mentioning "The Engineers' Digest" as a source.

- NEW EQUIPMENT
- BOOKS AND CATALOGUES
- BUSINESS CHANGES
- PERSONAL
- NOTES

NEW HACKSAWING MACHINE.

It is claimed that original features are incorporated in a new hacksawing machine that is being marketed by Broadway Engineering Co. Ltd. and, incidentally, it is the first of a range of new machines designed by this firm.

The saw bow of the machine is a semi-steel casting guided to the bow frame by two wide dove-tailed guides with adjustable taper gibs for taking up wear.

A single lever adjacent to the starter buttons controls the hydraulic operation with three positions, lower, run and rise. At "lower" the saw is lowered gently on to the work. At "run" the cutting is performed on the pulling stroke, while on the return the frame is lifted to relieve pressure on the blade. At "raise" the frame is rapidly lifted and is held on the top position by a safety latch, while at the same time the motor is automatically cut out by a limit switch.

Cutting pressure on the machine is adjustable by a handwheel conveniently located at the front end of the machine. The amount of pressure is indicated by a sliding pointer, which feature enables variations of pressure to be made according to the shape and tensile strength of the material to be cut. An adjustable choke valve is incorporated which permits the amount of penetration of the saw during the cutting stroke to be controlled.

With regard to the drive this is taken from a 2 h.p. motor mounted in the base of the machine by three Vee belts to a gear box giving cutting speeds of 90 and 162 strokes per minute. The lower speed is for ferrous and the higher speed for non-ferrous metals. There is, of course, push button control.

The vice, which can be completely removed from the bed, may be swivelled for angular settings up to 45 degs. With the vice removed there are tee slots for the reception of special work-holding fixtures. A coolant system is incorporated as standard equipment and the bed is so designed that coolant falls through a wide slot into the sump while swarf is collected in a tray.

The round capacity of the machine is 12 ins. and its overall weight 15¼ cwts. It occupies a floor space of 4 ft. 9 ins. × 2 ft. 6 ins.

PATENT CLAMP.

We have received particulars of an interesting new patent Camclamp from Messrs. Dean & Mulhall Ltd., of 27, Sidney Street, Sheffield, who are specialists in rapid methods of holding work in jigs and fixtures.

It is primarily intended for the instantaneous holding of work on jigs and fixtures of all kinds. Outstanding features include a reversible action which eliminates vibration or chatter, and lightness in operation which makes it suitable for female operatives.

The hardened curved surface of the specially developed cam has a rise of one thou. per degree. The hardened pin which makes line contact with the cam will effectively clamp anywhere between two points at 45 degrees on either side of the vertical centre line so that the work to be held can vary in thickness up to .090" and still be clamped without adjustment.

The cam is spring loaded for fly-back release and a stop pin ensures that the knob cannot be moved back too far, thus avoiding the risk of breakage.

There is ample clearance from the base to the under-side of the cam and from the clamping pin to the near side of the base bracket. The compactness of the design ensures that the clamp can be used for nearly every job which would normally use the spanner type of clamp.

Although the clamping pin itself is sufficient for the majority of jobs the user can readily fit different kinds of clamping or locating plates to the clamping pin if necessary.

REPAIRING DAMAGED CABLES.

Conservation of all articles using rubber is now of prime importance, yet cable is being subjected to much heavier wear and tear under the present intensive production conditions. One of the most difficult forms of damage is the invisible break and in this connection it is interesting to note that the B.C.E. Cable Break Locator marketed by British Central Electrical Co. Ltd., 6-8 Rosebery Avenue, London, E.C.1, enables broken conductors to be located in a few minutes by external means and is particularly useful where the insulation shows no external damage. The instrument is simple to use and can be operated by inexperienced persons. The Cable Break Locator is portable so that the cable can be tested on site in the works, the change of volume in a telephone indicating the position of the break, while for exceptionally noisy places an amplifier is available.

Another useful apparatus is the H.F. Vulcanizer, which has been developed by the same firm in conjunction with Harvey Frost & Co. This vulcanizing device enables repairs to be made in anything from 20-60 minutes, depending on the size and nature of the cable to be treated. The Vulcanizer is not limited to repair of cable and can be used for vulcanizing such articles as damaged hose, inner tubes, covers, valve seatings, etc.

HEAT TREATMENT SPECIALISTS

ON APPROVED LIST OF AIR MINISTRY AND ADMIRALTY

- Case Hardening and straightening up to 8 ft. long.
- Hardening all Classes of Sub. and High Speed Steel Tools, Bakelite Moulds and Press Tools.
- Hardening by the Shorter Process.
- Cyanide Hardening, Capacity 3 tons per week
- Springs: Any size, shape or quantity.
- Aluminium Alloys Heat Treated to A.I.D. Specifications.
- Heat Treatment of Alloy Steels up to 10 ft long
- Heat Treatment of Meehanite Castings, etc.
- Crack detecting on production lines.
- Chemical blacking to A.I.D. Specification.

THE EXPERT TOOL & CASE HARDENING CO. LTD.
(Est. 1918)
Phone LIBERTY 2273-4
MORDEN FACTORY ESTATE : LONDON : S.W. 19
And GARTH ROAD, LOWER MORDEN, SURREY.
Telephone: Derwent 3122

GRAIN SIZE IN TIN ALLOYS.

THE effect of grain size on the physical properties of metals has been studied by various research workers. Interesting light on the part played by grain size in the properties of pure tin and tin-rich alloys is given in the Tin Research Institute's publication No. 118, which is a reprint of a paper by Dr. W. T. Pell-Walpole in the Journal of the Institute of Metals.

Dr. Pell-Walpole's investigations show that variations in tensile strength are controlled by the number of grains in the cross-section, and not by the absolute grain size. In rolled material, an increase in tensile strength is observed as the number of grains in the cross-section increases from 1 to 20 or 30. Elongations are constant over this range. A further reduction in grain size produces only a slight increase in tensile strength, but elongations increase rapidly.

The discontinuity in the relationship between tensile strength and grain size is shown to be caused by the corresponding discontinuity in the extension/grain size curve, the latter having some fundamental cause. The calculated true stress was found to vary continuously with grain size.

With chill-cast specimens, consisting entirely of columnar grains, tensile strengths increase continuously with reduction of grain size, and elongations are either constant or increase only slightly.

Copies of this publication may be obtained free of charge from the Tin Research Institute, Fraser Road, Greenford, Middx.

THE BRITISH INSTITUTION OF RADIO ENGINEERS.

AT the meeting held on the 21st May, the following elections and appointments have been made for the year 1943/4: Sir Louis Sterling, President; Air Vice-Marshal R. S. Aitken, D.F.C., Vice-Admiral the Lord Louis Mountbatten, G.C.V.O., D.S.O., A.D.C., A.M.I.E.E., R.N., H. Leslie McMichael, M.I.E.E., Sir William Noble, M.I.E.E., and James Robinson, M.B.E., Ph.D., D.Sc., M.I.E.E., Vice-Presidents, and L. Grinstead, M.I.E.E., Sir Arrol Moir, Bart., B.A., M.Inst. C.E., N. W. McLachlan, D.Sc., L. H. Bedford, O.B.E., M.Sc., A.M.I.E.E., W. E. Miller, M.A., M.I.E.E., N. Partridge, Ph.D., M.I.E.E., J. A. Sargrove, A.M.I.E.E., W. W. Smith, B.Sc. (Hons.), A.M.I.E.E., G. A. V. Sowter, B.Sc., M.I.E.E., Squadron Leader S. R. Chapman, M.Sc., J. Dimmick, B.Sc., and Lt.-Colonel P. Northey, Members to serve on the General Council of the Institution.

PERSONAL.

Sir A. Stanley Angwin has been elected President of the Institution of Electrical Engineers for 1943-44. **Mr. T. G. N. Haldane** and **Dr. E. B. Moullin** have been elected Vice-Presidents.

Sir Edward Appleton, K.C.B., M.A., F.R.S., and **Mr. H. R. Ricardo,** B.A., F.R.Ae.S., M.I.A.E., M.I.Mech.E., F.R.S., have had conferred upon them honorary degree of Doctor of Laws of the University of Birmingham.

Mr. L. F. G. Butler has been appointed technical adviser of the Aero-Engine Division of the Bristol Aeroplane Co. Ltd.

Major-General G. Cheetham, D.S.O., M.C., has been appointed Director-General of the Ordnance Survey.

Mr. E. L. Denny has been appointed Director of William Denny and Brothers, Ltd., Dumbarton.

Mr. W. P. Digby, M.I.E.E., M.I.Mech.E., has died recently.

Mr. T. E. Goldup has been appointed Chairman, and Professor Willis Jackson, D.Sc., D.Phil., Vice-Chairman of the Wireless Section of the Institution of Electrical Engineers.

Mr. E. Hallas has been appointed technical sales manager to the Brightside Foundry and Engineering Co., Ltd.

Mr. Willard F. Jones has been elected President of the American Committee of Lloyd's Register of Shipping.

Mr. F. W. Lawton has been appointed Chief Engineer and Manager of Birmingham Corporation Electric Supply Department.

Mr. P. A. Leggett and Mr. A. H. Leggett have been appointed Directors of Bull Motors (Branch of E. R. and F. Turner, Ltd.), Ipswich.

Mr. S. Mavor of the firm Mavor & Coulson, Ltd., Glasgow, has died recently.

Mr. W. E. Sykes, Founder of the firm of W. E. Sykes, Ltd., Manufacturers of gear-cutting machines and high-precision instruments, Staines, Middx., has died recently.

Mr. W. T. Tolhurst has been appointed Director of W. G. Allen and Sons (Tipton), Ltd.

The Hon. Edward Pearson Warner has been elected an Honorary Fellow of the Royal Aeronautical Society.

Mr. Reginald Woods has been appointed Managing Director of General Cable Manufactg. Co., Ltd., Leatherhead.

CATALOGUES RECEIVED.

MONOMETER FURNACES.—The Monometer Manufacturing Co., Ltd., has issued a 4-page leaflet illustrating the wide range of Crucible and Non-crucible type Melting Furnaces, and the White Metal Melting and Pressure Casting Plants which form the production program of that firm. Copies of the leaflet are available upon request from the Monometer Mfg. Co., Ltd., Green Lane, Braughing, Herts.

Change of Address:—The Broadway Engineering Co., Ltd., has changed the address of the Head Office to Watford-by-Pass, Herts.

METALLIC BELLOWS

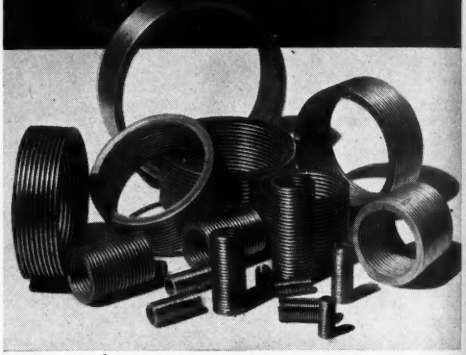

for Instruments of Precision

PACKLESS GLAND CO. LTD.

WINDMILL ROAD, SUNBURY-ON-THAMES, MIDDLESEX

Telephone: SUNBURY-ON-THAMES 459 (6 LINES)

UNIVERSAL ME PATENT BALL JOINTS

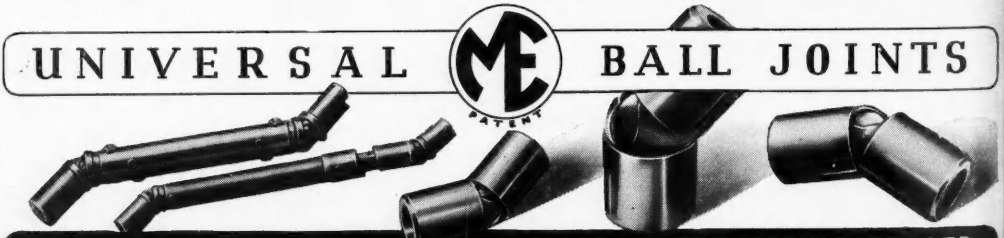

Made in a range of nine sizes for shafts from ¼" to 1⅝" diameter.
Efficiency 92% to 98%. N.P.L. Certified. Catalogue on request.

MOLLART ENGINEERING CO. LTD.
KINGSTON BY-PASS, SURBITON, SURREY.
Telephone: ELMBRIDGE 3351-3-4-5. Telegrams: PRECISION, SURBITON

es, Ltd.,
instru-

G. Allen

cted an

Director

ufactur-
le range
e White
produc-
le upon
Braugh-

td., has
, Herts.

S

n

CO.
LTD.
SEX